



## Introduction

The ISOLDE experimental campaign 2011 was highly successful. Forty-nine experiments and as many as 8 test runs were scheduled, which collected data using over 90 different beams. The number of shifts delivered increased by 20% over 2010. As you will read among the highlights presented in this newsletter, a first production run on  $^{35}\text{Ar}$  for WITCH was successful. The mass and half-life measurement of  $^{82}\text{Zn}$  with ISOLTRAP is a result of importance both for nuclear structure and for astrophysics. On the laser spectroscopy front COLLAPS was used to collect new data on the spins, radii, and moments of light  $^{63-70}\text{Ga}$ , neutron-rich  $^{51}\text{K}$ , and heavy Cd isotopes, while CRIS obtained the first laser-spectroscopy results on neutron-deficient Fr isotopes, opening a path towards laser spectroscopy with very weak beams. MINIBALL studied Coulomb excitation of  $^{98}\text{Sr}$ ,  $^{128}\text{Cd}$ , and light Pb isotopes, and two-neutron transfer reactions on  $^{66}\text{Ni}$  and  $^{72}\text{Zn}$ , extending to these heavier nuclei the methods developed in previous years and preparing to take advantage of the capabilities of HIE-ISOLDE. Beautiful COULEX results on octupole collectivity were obtained for  $^{220}\text{Rn}$  and  $^{224}\text{Ra}$ , post-accelerated beams unique to REX-ISOLDE. The solid state studies covered diffusion in semiconductors and metallic compounds and online emission-channelling studies using  $^{27}\text{Mg}$  and  $^{65}\text{Ni}$  as probes. Perturbed angular correlation was used in biophysics studies with  $^{199\text{m}}\text{Hg}$  on proteins and bacteria, and for local probing on graphene and fullerenes. Mössbauer spectroscopy on  $^{119}\text{In}$  clarified some conflicting results in the literature, while Tb isotopes from ISOLDE were tested for diagnosis and therapy at PSI. Several ISOLDE results were published in letter journals including the charge radii

measurements of  $^{21-32}\text{Mg}$  and  $^{12}\text{Be}$  and the COULEX of  $^{96}\text{Kr}$ , which confirmed the previous results of ISOLTRAP and COLLAPS pointing to a smooth onset of deformation in neutron-rich Kr isotopes. You will also read about the continued R&D on targets and ion sources which is indispensable to ensure the pre-eminence of ISOLDE as a world-leading ISOL facility.

In order to maximise the amount of beam delivered before the long shutdown of 2013, last winter's shutdown was shortened and physics runs started up successfully at the beginning of April, with REX getting into the action during the first week of May. In the coming months up until the first week of December, we will witness experiments with devices new to ISOLDE, including the active target MAYA from GANIL, an optical TPC from Poland and the realization of the first resonant scattering experiments making use of the reaction chamber provided by our Swedish colleagues. Last November, two new research fellows were hired for ISOLDE, Susanne Kreim for ISOLTRAP and Elisa Rapisarda for MINIBALL. Jan Kurcewicz, a fellow funded by the ENSAR contract, who joined ISOLDE last December is devoting a large part of his time to the upgrade of the data acquisition at ISOLDE.

HIE-ISOLDE is rapidly becoming reality as civil engineering work started last year. The entrance to the hall has been moved and the cryo-plant and ventilation buildings are taking shape. Performance of the sputtered cavities is reaching the design goal. The move of the TSR storage ring from Heidelberg to ISOLDE was presented to the INTC through a detailed TDR which was enthusiastically endorsed. We now have to lobby for approval of funding for the necessary building which would be located behind the ISOLDE hall on the "Jura side". The group of the University of York has secured a used MRI solenoid which could

form the basis of a light particle spectrometer for transfer reactions, akin to the HELIOS experiment at Argonne. After the summer the INTC will call for proposals for the first stage of HIE-ISOLDE at 5.5 MeV/u. We expect an overwhelming response from scientists from our 15 collaboration states, including our most recent and largest member India, which signed the ISOLDE MOU during a dedicated workshop organised in Kolkata in April.

The long shutdown will present an opportunity to reflect on our long term future, and to get involved in related initiatives. In its long range plan published in 2010, NuPECC endorsed the construction of EURISOL as the most important long term priority for low energy nuclear physics in Europe. You may not be aware that ISOLDE and CERN, after having been among the major players of the EURISOL Design Study, rapidly acted on this recommendation. We are leading the EURISOL-NET network in ENSAR, a work package in the TIARA preparatory phase contract devoted to designing a test stand for the EURISOL high power target and this month was the first meeting of a broad collaboration which has formed around an initiative taken by our target group to build and test a Pb-Bi loop at ISOLDE. Whether EURISOL is eventually sited at CERN or elsewhere, it will only succeed with a major investment of the ISOLDE user community and technical groups. Please consider attending the EURISOL topical and town meetings in Lisbon in October to learn about the ongoing initiatives and demonstrate your support for our future facility.

This is the last time I write the introduction to the newsletter as I will be returning to Orsay in August. I thank all of you for making my time at ISOLDE so exciting and enriching. I have done my best to contribute to ensuring the recognition and

development of our science at CERN. I am pleased to leave the Physics group in the expert hands of Maria J. G. Borge, who will take on the exhilarating and challenging task of leading the start up of the HIE-ISOLDE physics program. I will continue to serve ISOLDE as chairperson of the Collaboration Committee and look forward to following the continued progress of this world class facility!

*Yorick Blumenfeld*

## Information for Users:

### **Responsibilities of Spokespersons**

This year we have several new groups leading ISOLDE experiments. Let us use this opportunity to remind you that being a spokesperson of an ISOLDE experiment carries with it some responsibilities.

Please make sure that all necessary equipment to perform your experiment is transported in time to ISOLDE or is reserved for you at ISOLDE (electronics, power supplies, detectors, roughing and turbo pumps, mechanical tools, vacuum elements). Contact us in advance if you require any of the common equipment. There were recently complaints from several fixed experiments that they were used as a pool of equipment for other setups.

Once your experiment is scheduled, check who will participate in it and whether their institute is part of your proposal (which can be verified via [Greybook](#)). If it is not, contact Jenny at the ISOLDE User Support Office and enquire how to add the institute to your experiment. Otherwise your colleagues will not be able to register. You can use this graphic "[ISOLDE access](#)" file as guidance.

Make sure that all participants of your experiment know the rules for registering as

CERN user and are aware of the requirements for obtaining a dosimeter and then access to ISOLDE. Again, the graphic "[ISOLDE access](#)" should be a good start.

Also, the participants should have at least a basic knowledge of ISOLDE and each shift should be led by somebody with a reasonable knowledge of the facility (preferably somebody who recently followed an ISOLDE separator course). Such a "shift leader" is the person communicating with the ISOLDE and booster operators.

## Registration and access to ISOLDE

As mentioned in the previous section, our graphical "[ISOLDE access](#)" contains a summary of how to register as a CERN user and how to obtain access to ISOLDE. Important reminder: the minimum period of your registration has to be one month, even if you stay only for a few days.

## Accident insurance

If you require an additional accident-at-work insurance, there are two affordable offers that covers the risk of death and disability (they do not cover medical expenses). These are the [HELSANA insurance and UNIQUA Accidenta](#).

## CERN Hostel booking

Following last years problems with CERN hostel availabilities, for this year we have negotiated a block booking of 10 rooms available for people on shift during the full running period. For practical reasons, the booking requests should be grouped by the spokespersons and communicated to me. Please use this group booking only when you couldn't book the room in the regular way.

## Free CERN bike and car sharing

A new bike sharing scheme allows using free-of-charge bicycles even in the summer peak season. The bikes are stationed in front of the CERN reception and can be used between 8h and 19h. When you show a proof of accommodation outside CERN you can also use them overnight to get to your hotel. For details, check [here](#).

The free-of-charge CERN car sharing scheme is now available for all CERN employees and users. There are 13 locations where the cars are available and the rental can now take place inside and outside the working hours. It might help you move around and between the CERN sites. However, "the use for personal purposes, such as travel between the place of residence and the work place, is strictly prohibited". Thus, you cannot take the car to go to your hotel. Check [here](#) for details.

*Magdalena Kowalska*

## News on data acquisition software and hardware

The Isolde DAQ based on XIA DGF-4C CAMAC modules is operated now from a new computer (pcepisdaq5). The new node offers a much higher operation speed and sufficient disk space.

A new oscilloscope LeCroy Wave Jet 354 is available for general use. It offers a 500 MHz bandwidth and up to 2 GS/s sampling rate (interleaved). The device has four input channels (Input Impedance  $1\text{ M}\Omega \pm 1.5\%$  ||  $16\text{ pF}$ ,  $50\ \Omega \pm 1.5\%$ ) and a 7.5" color display.

Two VME Universal Logic Modules VULOM 4B have arrived recently. The VULOM-based trigger logics replaces several crates of NIM and CAMAC electronics used for trigger decisions, counting and dead-time locking. It is possible to use them for various

purposes by replacing logic on the FPGA. Presently the modules are being installed and tested with the MBS DAQ system.

The single crystal Canberra-Eurysis Ge detector equipped with a beryllium window has returned from repair and is again available for general use.

If you wish to use any of the above equipment, contact:

*Jan Kurcewicz*

## Neutron-wall

With this note we would like to investigate the interest for using the neutron-wall of the European gamma-ray spectroscopy pool in an experimental campaign at ISOLDE after the long shutdown of 2013.

The neutron wall consists of 50 liquid scintillator detectors that can be used in a closely packed geometry covering a solid angle of approximately  $1\pi/\text{sr}$  but potentially also in other geometries. In the closely packed configuration the distance from the center of the set-up to the detector surface is 50 cm. The thickness of the detectors is 15 cm. The detectors use pulse shape discrimination in order to separate neutrons and gamma-rays. As part of the European gamma-ray spectroscopy pool the detector is available for experimental campaigns at European accelerator laboratories. The n-wall is managed by the nuclear structure group at Uppsala University and is currently located at GANIL. If you are interested in learning more about the possibilities of the n-wall please contact Johan Nyberg at Uppsala University. If sufficient interest is found we will submit an application to the owners committee of the gamma-ray pool for a campaign at ISOLDE.

Visit <http://nsg.physics.uu.se/nwall> for more information about the n-wall or send an e-mail to johan.nyberg at [physics.uu.se](mailto:johan.nyberg@physics.uu.se)

*Joakim Cederkäll*

## Experiment reports:

### IS413: High-Precision Mass Measurements of n-rich Zinc Isotopes

In 2011, the ISOLTRAP collaboration succeeded in performing the first mass measurement of  $^{82}\text{Zn}$ , the most exotic nuclide at the  $N=50$  shell closure. The major challenge in this region of the nuclear chart, contaminations from rubidium isotopes, was overcome by applying all state-of-the-art purification techniques available at both, ISOLDE and ISOLTRAP: At ISOLDE, instead of directly irradiating the target, a neutron converter was used, furthermore a quartz transfer line suppressed unwanted ions, and finally resonant laser ionization with RILIS further increased the ion-of-interest to contamination ratio. At ISOLTRAP (see report on IS 518 by M. Rosenbusch for a detailed experimental description), the recently integrated MR-TOF mass separator [1,2] acted as the main device for contamination removal. In contrast to the standard cleaning in the preparation Penning trap it allows the removal of contaminations within only a few milliseconds. The position of the center of the resonances of  $^{80-82}\text{Zn}$  were determined by the conventional time-of-flight ion-cyclotron resonance (ToF-ICR) method (Fig. 1 left) and by use of the Ramsey excitation scheme (Fig. 1 right), resulting in a relative uncertainty of  $4 \cdot 10^{-8}$ . Furthermore, the life time of  $^{82}\text{Zn}$  was measured by monitoring the decay during storage in ISOLTRAP's first trap, the RFQ buncher. The data are under evaluation.

On the one hand, the low uncertainty of  $10^{-8}$  allows for the most exotic test yet of  $N=50$  shell gap. On the other hand, the mass of

$^{82}\text{Zn}$  is important in the context of stellar nucleosynthesis, in particular for modeling the  $r$ -process path [3], and can be used to probe the elemental composition of the outer crust of neutron stars [4].

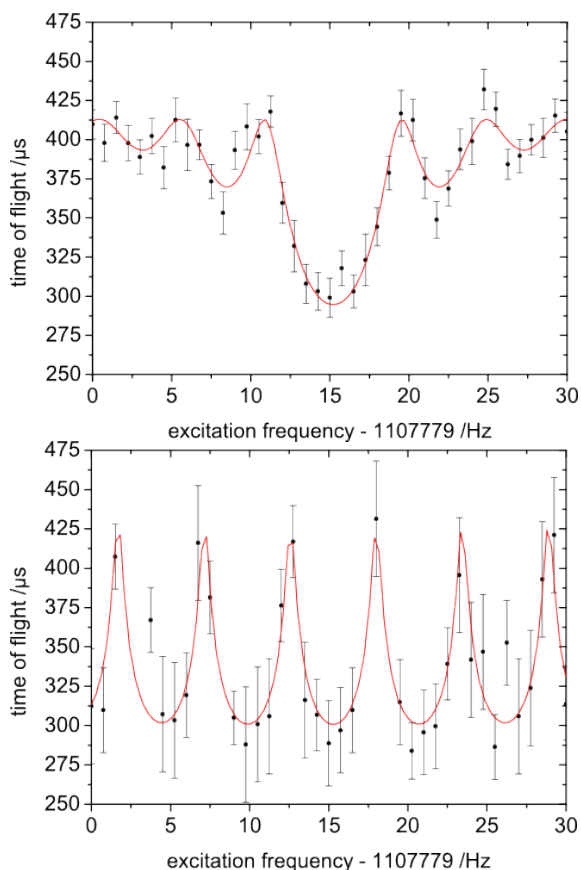


FIG. 1: Conventional ToF-ICR (left) and Ramsey-excitation resonance (right) of  $^{82}\text{Zn}$ . The red lines show a fit of the expected resonance curves to the data.

[1] R.N. Wolf et al., *Hyperfine Interact.* 199 (2011) 115.

[2] R.N. Wolf et al., *Int. J. Mass Spectrom.* 313 (2012) 8.

[3] S. Baruah et al., *Phys. Rev. Lett* 101 (2008) 262501.

[4] S. Goriely et al., *A&A* 531 (2011) A78.

*R. Wolf for the ISOLTRAP Collaboration*

## IS433: First data sets on $^{35}\text{Ar}$ acquired with the WITCH experiment

Low energy precision experiments searching for exotic components in the weak interaction are complementary to the high energy experiments at colliders dedicated to discover new particles. In the WITCH experiment the beta neutrino angular correlation coefficient ( $a$ ) in the beta decay of  $^{35}\text{Ar}$  is studied to search for a possible admixture of a scalar weak interaction component.

The WITCH setup [1,2] is situated behind REXtrap getting pre-cooled bunches of up to  $1 \cdot 10^6$  ions. The ion bunch is transferred through the horizontal and vertical beam lines to the WITCH Penning traps. In the first trap the ion ensemble is further cooled and centered by interaction with a buffer gas environment. After transfer to the second trap the ions are stored there under UHV conditions and left to decay. In the decay process the ions receive recoil energy allowing them to leave the trap. Half of the ions travel upwards through the spectrometer where almost all their energy is converted into axial energy which is then analyzed by a blocking potential in the retardation spectrometer. A spectrum is recorded by counting the number of ions reaching the main detector as a function of time, i.e. voltage.

2011 was a very successful year for the WITCH collaboration! After a first test with  $^{124}\text{In}$  [3], several upgrades [4-6] had been implemented to remove a number of observed disturbing effects and to improve the quality of the WITCH operations. It was finally possible to acquire first data on the prime physics case of  $^{35}\text{Ar}$ . Although in a first experiment, in June, only a few thousand counts were recorded, this still allowed reconstructing the recoil energy distribution of the daughter nuclei  $^{35}\text{Cl}$ . This

very preliminary spectrum was investigated with the help of software packages developed in our collaboration [7,8]. Although the achieved precision on  $a$  was still limited [9] it demonstrated the full operability of the setup.

A second online experiment was performed at the end of October. Despite of problems with the ISOLDE target and with the transmission between REXtrap and the WITCH cooler trap significantly higher statistics was acquired. It was, however, not yet sufficient to study systematic effects. Fortunately another experiment could be performed within a week due to the efforts of the target group and the I88 collaboration offering their time slot.

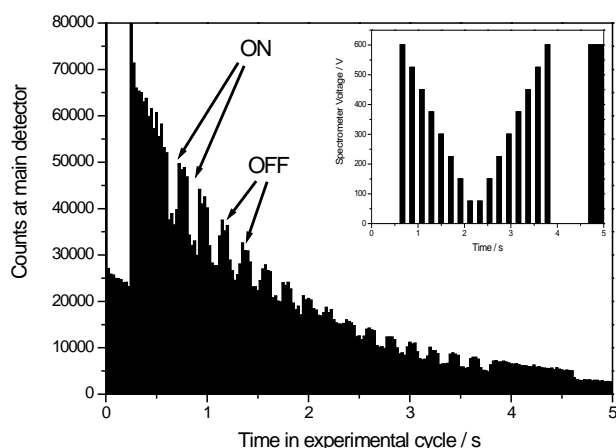


*Fig. 1: Detected ions on the main detector as a function of the time in the experimental cycle. The inset shows the applied retardation voltage in the spectrometer as a function of time. Peaks in count rate are observed when no retardation potential is applied ('OFF'), while dips indicate that recoil ions have been blocked by the retardation voltage that was applied ('ON').*

An example of an obtained raw spectrum is shown in Fig. 1. The number of counts on the main detector is plotted as a function of time. In the inset the applied retardation voltage is given as a function of the time in

the experimental cycle. Counts are missing, where a retardation voltage is applied in the spectrometer with respect to the undisturbed exponential decay, i.e. when no potential is applied. These missing counts are the events, which can be attributed to recoil ions. Since this spectrum contains more than  $10^5$  events a statistical uncertainty of less than 5% in the determination of the correlation parameter  $a$  should be reachable.

- [1] M. Beck et al., Nucl. Instr. Meth. A 503 (2003) 567.
- [2] V.Yu. Kozlov et al., Nucl. Instr. and Meth. B 266 (2008) 4515-4520.
- [3] M. Beck et al., Eur. Phys. J. A 47 (2011) 45.
- [4] M. Tandecki, PhD thesis, IKS, KULeuven (2011).
- [5] E. Traykov et al., Nucl. Instr. and Meth. 648 (2011) 1-14.
- [6] M. Tandecki et al., Nucl. Instr. and Meth. A 629 (2011) 396-405.
- [7] S. Van Gorp et al., Nucl. Instr. and Meth. A 638 (2011) 192-200.
- [8] P. Friedag, diploma thesis, IfK, University Muenster (2008).
- [9] S. Van Gorp et al. in preparation.

*M. Breitenfeldt*

## IS448 and I88: Metal ions in biology

The main objective addressed in both these projects is to explore the structural and catalytic role of metal ions in biological molecules. Understanding the manner in which certain metal ions bind to their biological ligands and activate them structurally, allows many crucial and, as-yet unanswered/unresolved issues, to be addressed, for instance: Is the structure of a protein dictated ONLY by the amino acids sequences or is it also steered by metal ions

– even for proteins that do not contain metal ions in their folded state? Studying the biochemistry of the most abundant metal ions in biology is actually as important as elucidating the toxicity of heavy metal ions, such as Hg(II), Pb(II) and Cd(II) at the molecular level. For the latter elements these matters *can be addressed* using PAC Spectroscopy. This technique cannot, however, stand alone and always has to be supported by other complementary techniques, such as UV-Vis, CD, NMR, EXAFS and fluorescence spectroscopies, as well as by quantum mechanical calculations of spectroscopic properties.

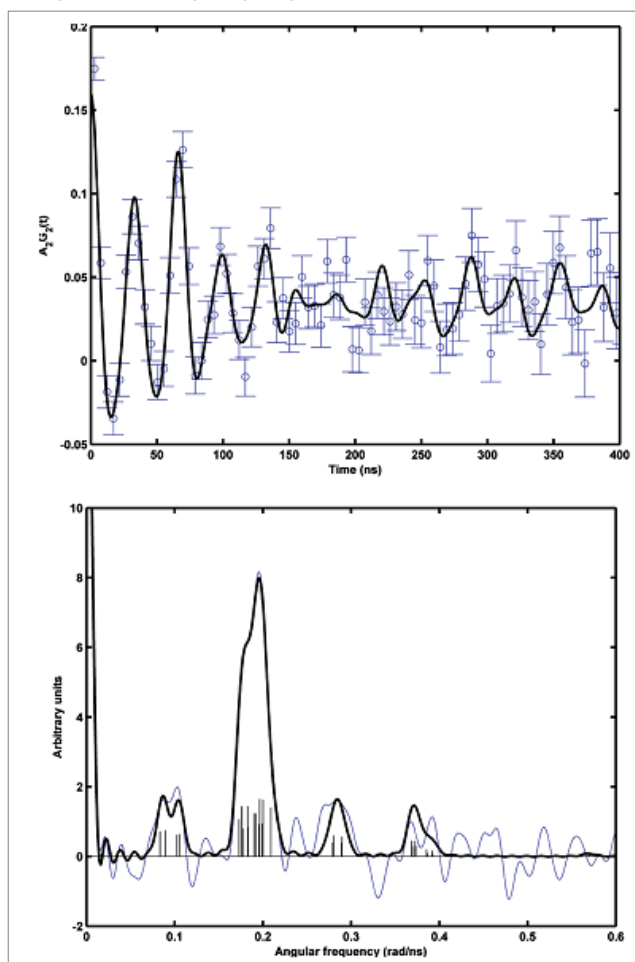


**Fig 1.** 204mPb-PAC spectra of powder crystals of  $[AsPh_4]_4[Pb(i-mnt)_4]$  (blue line: experimental data, black line: fit). Reprinted with permission from [1]

One of our achievements in the past year has been in describing the Pb(II) coordination compound:  $[AsPh_4]_4[Pb(i-mnt)_4]$ . The measured spectrum shown in Figure 1 represents the very first application of 204mPb-PAC to a Pb(II) molecular crystal with a known structure [1]. Electronic structure calculations (DFT), determined at the PW91/QZ4P level including relativistic effects using the two-component zeroth-order regular approximation method, agree reasonably well with the experimental data for the dimeric structure (Figure 2 right) but not monomeric as previously reported in the literature (Fig 2 left). Our findings are providing valuable information on the coordination chemistry geometry of Pb(II), and thus contributing to a better understanding of how and where the lead ion binds to bio-molecules.

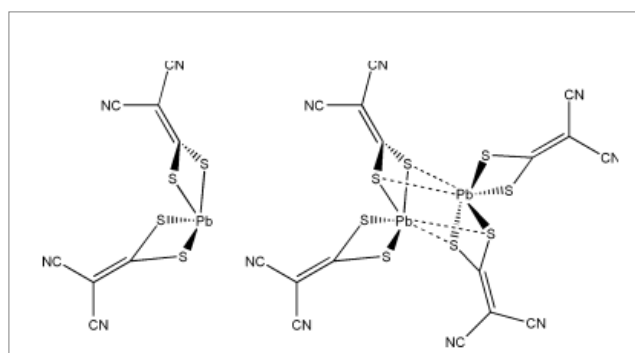


**Fig 2.** Models of  $[AsPh_4]_4[Pb(i-mnt)_4]$ . Reprinted with permission from [1]

The second of our projects, I88, aims to set up the world's first  $\beta$ -NMR instrument designed for biophysics applications.  $\beta$ -NMR is a technique where NMR resonances are observed as changes in the  $\beta$  decay anisotropy. It has already been successfully applied in solid state and nuclear physics and the technique also holds great promise for successful applications in biology, although no such experiment has yet been performed on soft matter. The underlying basic physics is the same as for NMR spectroscopy on stable isotopes, thus,

knowledge built up over the last decades for NMR may be transferred to  $\beta$ -NMR applications. This project is motivated by the need to find a new spectroscopic approach to study electronically and magnetically silent metal ions, such as Mg(II), Ca(II), Zn(II) and Cu(I), some of the most essential ions in biology.

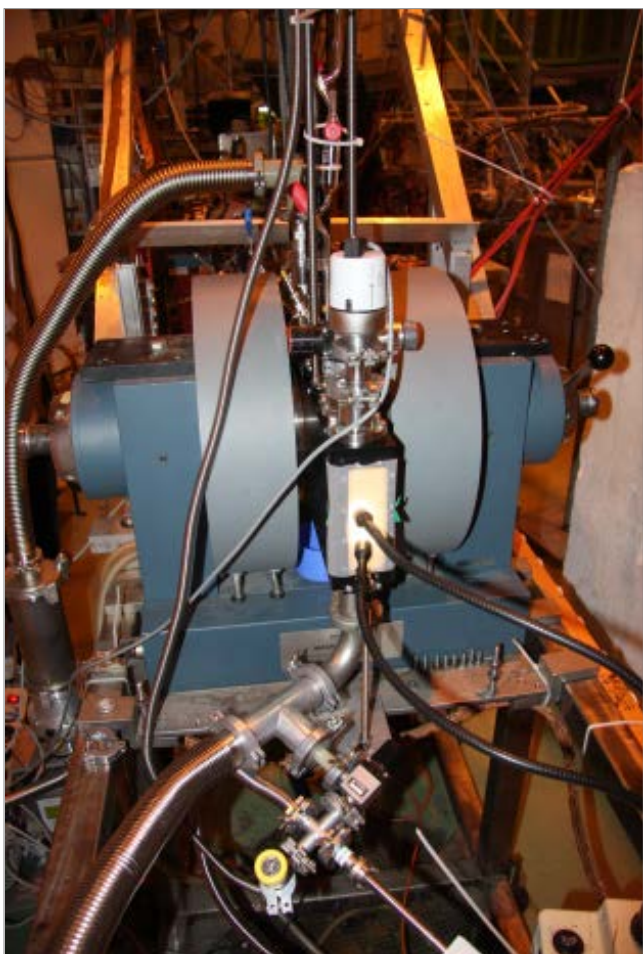


**Fig 3.** *The bio-setup at the COLLAPS magnet*

In November 2011 the first on-line tests with a stable Mg(II) beam took place, in which we demonstrated a fully working and ready-for-radioactive-beams experimental setup. The system, illustrated in Figure 3, was assembled at ISOLDE and tested at the COLLAPS beam line. The tests showed that the sole remaining issue is low beam transmission through the array of 3x4mm

pin-holes. For this year's run, however, we believe we can improve the experimental conditions by using so-called ionic liquids as our targets, which have negligible vapor pressure and therefore are ideal for our purpose.

[1] Vibenholt et al, "Application of 204mPb Perturbed Angular Correlation of  $\gamma$ -rays Spectroscopy in Coordination Chemistry" accepted for publication in *Inorganic Chemistry*, 2012

*M. Stachura on behalf of IS448, IS488 and I88 collaborations*

### **IS453: Minority-site occupancy of transition metals in dilute magnetic semiconductors**

For the EC-SLI collaboration, 2011 marked the end of an important chapter on the lattice location of transition metals in *dilute magnetic semiconductors*. Unexpected results from the experimental runs of 2007-2009, which required careful validation by experiments performed in 2010, finally came together in several publications (two of which were already published [1,2]).

In a *dilute magnetic semiconductor* (DMS), magnetic atoms (or *impurities*) are introduced in an otherwise non-magnetic semiconductor. For almost two decades, the co-existence of ferromagnetism and semiconducting behavior in some DMS materials has generated fundamental new physics and enabled the study of phenomena of interest for spin electronics (*spintronics*) [3,4]. The current research interest can be narrowed down to two main classes of materials: (1) *narrow-gap* III-V semiconductors, mostly GaAs, doped with Mn; (2) *wide-gap* oxides and nitrides doped

with 3d transition metals, mostly Mn-, Fe- and Co-doped ZnO and GaN. However, even these intensively studied DMS materials are still far from understood [4]. Some of the open questions are at the very basis of the DMS magnetism: the position (*site*) of the magnetic impurities in the host *lattice*. In general, it is easy to determine the lattice site occupied by the *majority* of the impurities. It is, however, far more challenging to identify lattice sites occupied by *minority* fractions which can, nevertheless, dramatically affect the magnetic behavior of the DMS.

*Emission channeling* (EC) overcomes several limitations of conventional techniques used to determine the lattice location of impurities in semiconductors. For  $\beta^-$  EC experiments performed with the short-lived isotopes  $^{56}\text{Mn}$  (2.58 h) and  $^{61}\text{Co}$  (1.6 h), IS453 makes use of the on-line EC-SLI setup, presently coupled to the GHM beam line. While  $^{56}\text{Mn}$  is available directly,  $^{61}\text{Co}$  is obtained by implanting the short-lived precursor isotope  $^{61}\text{Mn}$  and exploiting the decay chain  $^{61}\text{Mn}$  (4.6 s)  $\rightarrow$   $^{61}\text{Fe}$  (6 min)  $\rightarrow$   $^{61}\text{Co}$ .

In  $^{56}\text{Mn}$ -implanted GaAs, in addition to the majority substituting for Ga, we identified a significant fraction of the  $^{56}\text{Mn}$  impurities occupying tetrahedral interstitial sites with As nearest neighbors (Figs. 1 and 2a) [1]. The interstitial fraction is stable up to 400°C, with an activation energy for diffusion of 1.7–2.3 eV [1]. Substitutional  $^{56}\text{Mn}$  becomes mobile at higher temperatures ( $\sim 700^\circ\text{C}$ ), with an activation energy of  $\sim 3$  eV. Being difficult to reconcile with the general belief that interstitial Mn out-diffuses at  $\sim 200^\circ\text{C}$  with an activation energy of  $\sim 0.7$  eV [5,6], our findings have profound implications on the prospects for achieving higher Curie temperatures in Mn-doped GaAs, one of the major goals in the DMS field [4].

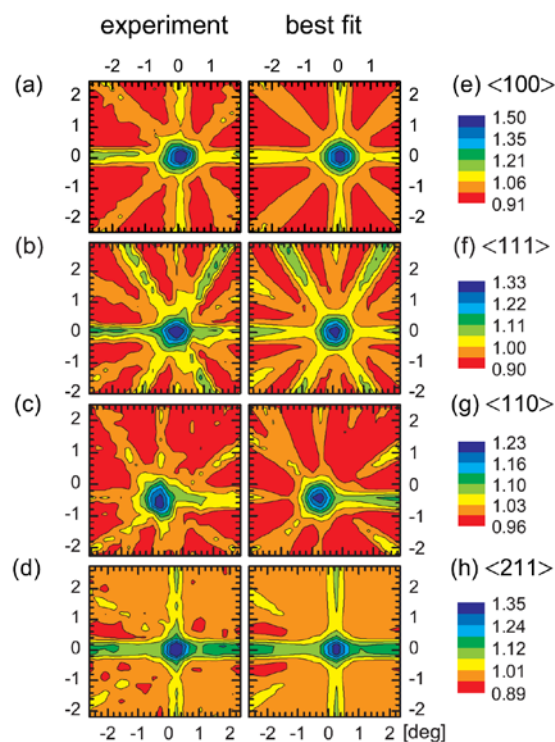


**Fig. 1:** (a)-(d) Normalized experimental emission channeling patterns (undoped GaAs) in the vicinity of the  $\langle 100 \rangle$ ,  $\langle 111 \rangle$ ,  $\langle 110 \rangle$  and  $\langle 211 \rangle$  directions following annealing at  $100^\circ\text{C}$ . (e)-(h) Corresponding best fits yielding 70% and 30% of the Mn atoms on Ga-substitutional and As-tetrahedral interstitial sites, respectively.

In  $^{56}\text{Mn}$ - and  $^{61}\text{Co}$ -implanted ZnO and GaN, in addition to the majority substituting for the host *cations* (Zn in ZnO and Ga in GaN), we identified significant fractions of the impurities occupying substitutional *anion* sites (O in ZnO and N in GaN), which are virtually unaffected by thermal annealing up to  $900^\circ\text{C}$  [2] (Fig. 2b). Anion substitution by Mn and Co impurities in wurtzite ZnO and GaN, which had never been observed before, challenges our understanding of transition-metal incorporation in wide-gap oxides and nitrides.

The magnetism community received very well the results of these two sets of emission channeling experiments. For an oral communication compiling these findings, Lino M. C. Pereira\* won the "Best

student presentation award" at the 56<sup>th</sup> Annual Conference on Magnetism and Magnetic Materials (November 2011, Scottsdale, USA), one of the most important conferences on magnetism and magnetic materials.

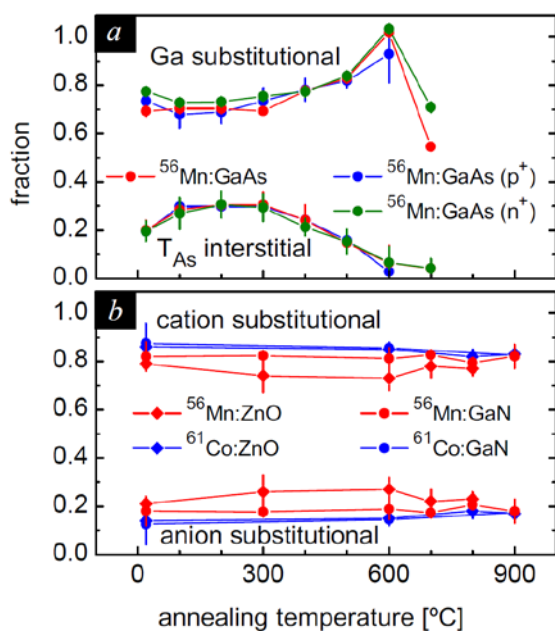


**Fig.2:** (a) Ga-substitutional and As-tetrahedral ( $T_{As}$ ) interstitial fractions of  $^{56}\text{Mn}$  in GaAs of different doping types. (b) Cation and anion substitutional fractions of  $^{56}\text{Mn}$  and  $^{61}\text{Co}$  in ZnO and GaN.

\*PhD student at IKS (KU Leuven) and IN-IFIMUP (University of Porto) until December 2011; currently a postdoctoral fellow at IKS.

[1] L. M. C. Pereira *et al.*, *Appl. Phys. Lett.* **98**, 201905 (2011)

[2] L. M. C. Pereira *et al.*, *Phys. Rev. B* **84**, 125204 (2011).

[3] A. H. Macdonald *et al.*, *Nature Mater.* **4**, 195 (2005).

[4] T. Dietl, *Nature Mater.* **9**, 965 (2010).

[5] K. W. Edmonds *et al.*, *Phys. Rev. Lett.* **92**, 037201 (2004).

[6] T. Jungwirth *et al.*, *Phys. Rev. B* **72**, 165204 (2005).

*U. Wahl, J.G. Correia, L. Pereira*

## IS463: Study of neutron-deficient Tl isotopes

Exotic ion beams produced at ISOLDE often consist of the ions of interest as well as isobaric and isomeric contaminations.

Thanks to its high resolving power of up to  $10^6$  the Penning-trap mass spectrometer ISOLTRAP [1] is able to resolve isomeric states even below 100 keV (for  $A \geq 150$ ) and thus can provide pure ion ensembles adequate for decay studies. Therefore, a trap-assisted decay spectroscopy setup was developed and installed at the end of the ISOLTRAP beamline [2]. It consists of an aluminized Mylar tape that is surrounded by a thin plastic scintillator sensitive to beta particles. Furthermore, two high-purity germanium detectors for gamma detection are in close proximity. All events are recorded by the ISOLDE digital data acquisition system allowing off-line reconstruction of coincidences.

In 2010, a series of mass and decay measurements was performed to study isomerism in the neutron-deficient thallium isotopes  $^{193-195}\text{Tl}$ . During this beamtime, the excitation energy of the first isomeric state in  $^{194}\text{Tl}$  was determined for the first time and the spin assignment of ground and isomeric state was confirmed. In 2011, ground and isomeric state in the even more exotic isotope  $^{190}\text{Tl}$  were investigated. It is known that there exist a  $2^{(-)}$  and a  $7^{(+)}$  state that differ in their decay pattern but their assignment to the ground and first isomeric state is still not clear. During this run, the mass of one of the states was determined with high precision and via the decay pattern the  $7^{(+)}$  state was assigned to it. A  $\gamma$ - $\gamma$ -coincidence spectrum of the two germanium detectors at the implantation point is shown in Fig. 1.

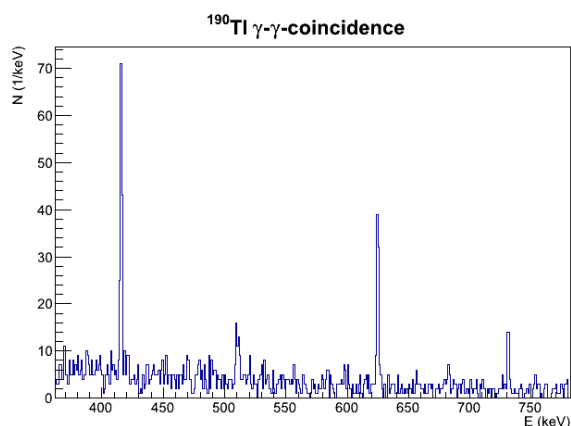


**Fig. 1:**  $^{190}\text{Tl}$   $\gamma$ - $\gamma$ -coincidence spectrum between the two high-purity germanium detectors at the implantation point.

[1] M. Mukherjee et al., *Eur. Phys. J. A*, 2008.

[2] M. Kowalska et al., *submitted to Nucl. Inst. and Meth. A*, 2011.

*J. Stanja for the ISOLTRAP Collaboration*

## IS471: Collinear resonant ionization laser spectroscopy of rare francium isotopes

In November of 2011, the CRIS beam line at ISOLDE performed its first collinear resonant ionization laser spectroscopy on  $^{207}\text{Fr}$ . This experiment marks the successful commissioning of the beam line [1]. A new decay spectroscopy station was also developed, and laser assisted decay spectroscopy was demonstrated in a collinear geometry.

This is the first experiment in a campaign to address several questions arising in the francium isotopes: the possible onset of shape coexistence in neutron deficient francium isotopes, the magnetic moment and isomer shift of the  $(n s_{1/2}^{-1})_{1/2}^{+}$  intruder state in  $^{201,203}\text{Fr}$  and the boundary of the region of reflection asymmetry in  $^{218,219}\text{Fr}$ .

In addition to the information provided by hyperfine measurements, decay spectroscopy can supply us with detailed information about the isomeric structure of  $^{202,204}\text{Fr}$  and its beta-delayed fission process.

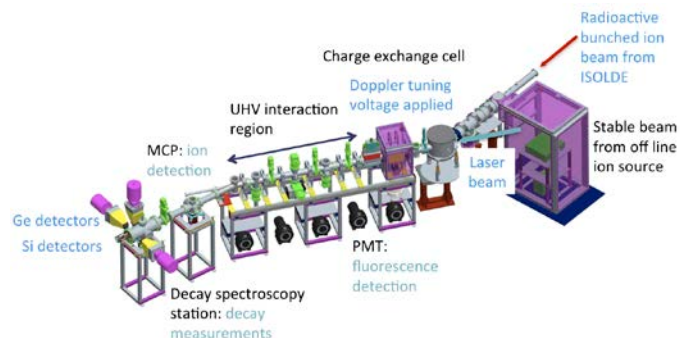
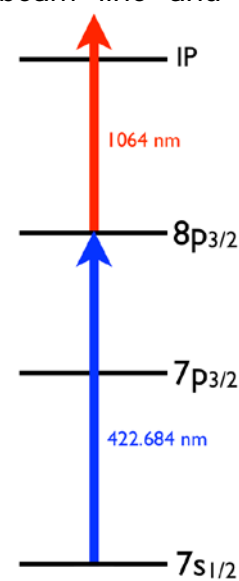


**Figure 1:** 3D drawing of the CRIS beam line and the decay spectroscopy station.

Figure 1 shows the CRIS beam line where laser radiation is used to step-wise excite and ionize an atomic beam using its characteristic hyperfine structure. In addition to hyperfine measurements, this technique offers the ability to purify an ion beam that is heavily contaminated with radioactive isobars, including the ground state of an isotope from its isomer [2], allowing decay spectroscopy to be performed.

A 30 kV bunched ion beam from HRS was deflected down the CRIS beam line and neutralized by a potassium vapour charge exchange cell, with an efficiency of  $\sim 50\%$ . A scanning voltage was applied to the neutralization cell, varying the velocity of the bunch, tuning it onto resonance with the laser. The resonantly produced ions were then deflected and detected with a MCP, or implanted in C-foils in the decay spectroscopy station. The ionization scheme for



francium consisted of a resonant (422nm) step from the  $7^2S_{1/2}$  ground state to the  $8^2P_{3/2}$  excited state [3], followed by a non-resonant 1064nm step into the continuum. A new laser system was developed for this purpose based on a tunable diode laser, which is pulsed amplified in a TiSa crystal [4]. The system was pumped by a 10Hz Nd:YAG laser, which was also used to provide the 1064nm ionization step. The collinear resonant ionization spectrum of  $^{207}\text{Fr}$  can be seen in Figure 2.

From a preliminary analysis of the experimental data, a value for the ground-state A-factor of  $A(S_{1/2})=8390(100)[200]$  MHz was found, which compares well with the literature value of  $A(S_{1/2})=8484(1)$  MHz [5]. The lower resolution obtained in this first run was due to power broadening of the 422 nm resonant step, which occurred while trying to optimize the overall experimental efficiency. In future experiments, this should be reduced, and the ionization efficiency should be enhanced by increasing the laser power of the 1064 nm non-resonant step by several orders of magnitude.

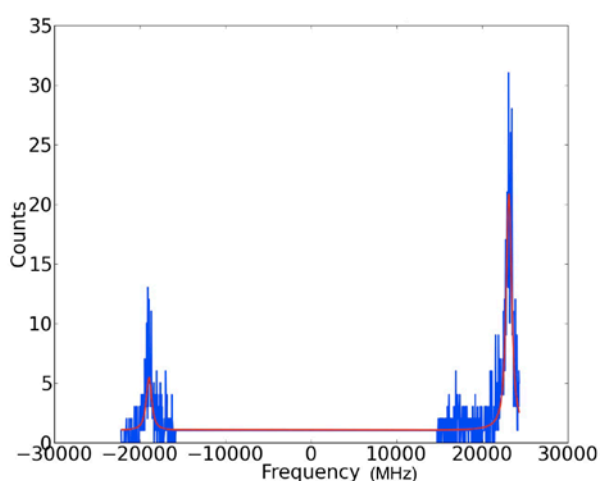


**Figure 2:** Collinear resonant ionization spectrum of  $^{207}\text{Fr}$ . Solid red line shows the fit to the experimental data.

The collinear geometry of the CRIS beam line gives a reduction in thermal Doppler broadening by a factor of  $\approx 10^3$ , thus the selectivity of the state of interest is greatly increased. The narrower line widths of the hyperfine transitions produced by the geometry lead to a greater degree of selectivity between the ground state and isomeric state of the isotope; thus decay spectroscopy on pure isomeric states can be achieved.

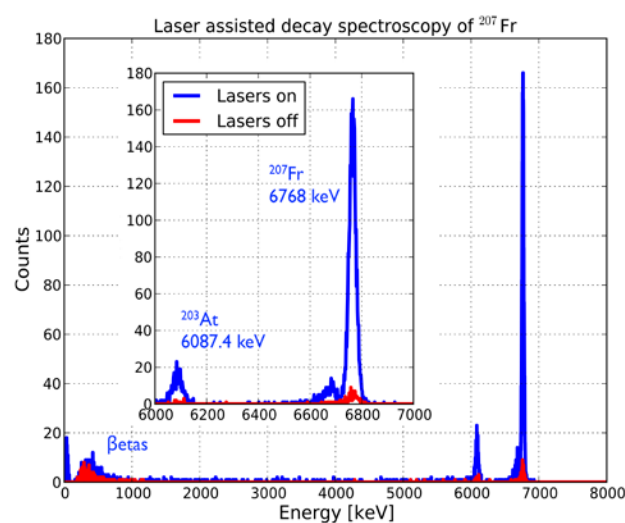


**Figure 3:** Alpha spectrum of the laser assisted decay spectroscopy performed on  $^{207}\text{Fr}$ .

Laser assisted decay spectroscopy was successfully performed on  $^{207}\text{Fr}$  during the IS471 run. Figure 3 shows the increase in the number of alpha particles detected when the laser was on resonance (blue spectrum) compared to when it had been blocked (red spectrum). The characteristic alpha particles emitted from  $^{207}\text{Fr}$  and its daughter  $^{203}\text{At}$  can be seen, giving an overall increase of a factor of 20 when the lasers are on. However, this result masks the low background rate (associated with collisional non-resonant ionization) due to the UHV conditions within the interaction region. The red line in Figure 3 could be further reduced by an order of magnitude by improvements in the vacuum (through

baking) to  $10^{-9}$  mbar; and additionally, the blue line could be increased by an increase in the resonant ionization efficiency.

The coming year will be spent improving the ion beam transport and resonant ionization efficiencies and then completing the study of the francium isotopes. The isotopes  $^{201-206,218,219}\text{Fr}$  will be studied with collinear resonant ionization spectroscopy; along with a detailed study with laser assisted decay spectroscopy of the isomers in  $^{202}\text{Fr}$  and  $^{204}\text{Fr}$ .

- [1] J. Billowes et al. CERN-INTC-2008-010. INTC-P-240 CERN, Geneva (2008)
- [2] V. Letokhov *Opt. Commun.* **7** 59 – 60 (1973)
- [3] H. T. Duong et al. *Eurphys. Lett.* **3** 175 (1987)
- [4] M. Hori and A. Dax *Opt. Lett.* **34** 1273 (2009)
- [5] A. Coc et al. *Phys. Lett. B* **163** 66 (1985)

*The authors would like to acknowledge the ISOLDE technical staff for their assistance during the experiment.*

*K.M. Lynch*

### **IS473: Q value for the double-beta decay nuclide $^{110}\text{Pd}$**

The hunt for the first detection of the neutrinoless double-beta decay is one of the most ambitious endeavours in particle physics [1]. Since the nuclide would decay by emitting only two electrons, the process would violate the law of lepton number conservation and is thus forbidden by the Standard Model of particle physics. On the other hand, it would only occur if the neutrino is its own antiparticle; a so-called Majorana particle. In addition, an observation of the neutrinoless double-beta

decay would lead to a determination of the unknown neutrino mass.

One key parameter in the design of a double-beta decay experiment is the Q value of the transition, i.e. the mass difference between the mother nuclide and the daughter nuclide. Its value defines the position of the characteristic single peak in the beta energy spectrum. Very few events are expected and thus, a precise determination of the Q value is of utmost importance to discriminate the signal from the background.

Only eleven nuclides have Q values high enough to allow the neutrinoless double-beta decay energetically and to reduce the expected half-life below the experimental limit. At the Penning trap mass spectrometer ISOLTRAP [2] at ISOLDE, the Q value of the candidate with the highest natural abundance,  $^{110}\text{Pd}$ , was determined with unprecedented accuracy.

The experimental setup consisted of the two ISOLTRAP Penning-traps and a laser-ablation source [3] for the off-line ion production of the mother nuclide  $^{110}\text{Pd}^+$  and its daughter nuclide  $^{110}\text{Cd}^+$ . Palladium and cadmium foils were mounted on a rotary sample holder to easily switch between the two isotopes. A 10 Hz frequency-doubled Nd:YAG laser was focussed on the samples for ablation and ionisation. The ion bunch was then purified by the preparation Penning trap with buffer-gas cooling and sent to the precision Penning trap, where the Ramsey time-of-flight ion-cyclotron resonance detection technique [4] was applied to determine its cyclotron frequency. See contribution of M. Rosenbusch for further details of the experimental setup. An example of an  $^{110}\text{Pd}^+$  resonance is shown in figure 1.

The Q value was determined from the cyclotron frequency ratio of  $^{110}\text{Pd}^+$  and  $^{110}\text{Cd}^+$  to be  $Q = 2017.85(64)$  keV [5]. This

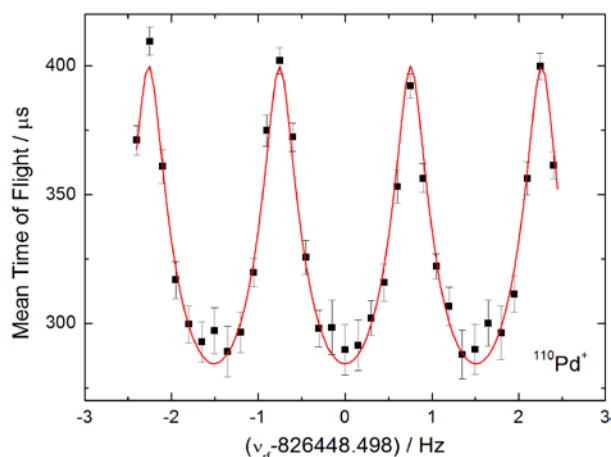


**Figure 1:** Ramsey time-of-flight resonance as a function of the excitation frequency for  $^{110}\text{Pd}^+$  with a fit of the expected line shape (solid line).

value is shifted by 14 keV compared to the previous literature value [6] and has a 17 times lower uncertainty. The new value is accurate enough to allow future experiments on neutrinoless double-beta decay to distinguish the experimental signal from the background. Moreover, the more precise Q value lead to a recalculation of the phase-space factors of the neutrinoless double-beta decay and its competing neutrino-accompanied mode, and thus to a new evaluation of both double-beta decay half-lives of  $^{110}\text{Pd}$  [5].

References:

- [1] K. Zuber, *Contemp. Phys.* 45, 491 (2004).
- [2] M. Mukherjee et al., *Eur. Phys. J. A* 35, 1 (2008).
- [3] K. Blaum et al., *Eur. Phys. J. A* 15, 245 (2002).
- [4] S. George et al., *Phys. Rev. Lett.* 98, 162501 (2007)
- [5] D. Fink et al., *Phys. Rev. Lett.* 108, 062502 (2012)
- [6] G. Audi, A. H. Wapstra, and C. Thibault, *Nucl. Phys. A* 729, 337 (2003).

*D. Fink for the ISOLTRAP collaboration*

## IS475: Octupole Collectivity – Coulomb Excitation of $^{224}\text{Ra}$ and $^{220}\text{Rn}$

The physics overview for this experiment was set out in last years ISOLDE Newsletter (2011) [1]. The aim of the experiment was to ascertain the strength of octupole correlations by measuring the E3 moments in nuclei where they are expected to be largest i.e. at  $Z = 88$  and  $N = 134$ . Here, there are a lack of spectroscopic data and so far, only for  $^{226}\text{Ra}$ , with its comparatively long half life of 1600 years, has it been possible to measure the  $B(E3)$  strength using Coulomb excitation [2].

Using the unique capabilities of ISOLDE to produce high intensity radioactive ion beams in the mass  $A=220$  region, and the ability of REX to accelerate these ions to 2.83 A.MeV,  $^{224}\text{Ra}$  was Coulomb excited by  $^{112}\text{Cd}$  and  $^{120}\text{Sn}$  secondary targets in inverse kinematics in 2010. The collaboration returned in 2011 to study  $^{220}\text{Rn}$  at 2.82 A.MeV using  $^{60}\text{Ni}$ ,  $^{114}\text{Cd}$  and  $^{120}\text{Sn}$  secondary targets.

The use of a much lighter target (changing  $Z$  from  $\sim 50$  to  $Z=28$ ) meant a significant change in the population of the states of interest in the nucleus, as can be seen in Figure 1. The lighter target reduces the Coulomb excitation cross-section for second-order processes and this allows one to disentangle the various excitation paths in the analysis, leading to a more precise measurement of the E2 and E3 matrix elements.

A new state was observed in  $^{220}\text{Rn}$  for the first time at 939keV. A similar state is also populated in  $^{224}\text{Ra}$ , which was previously observed in  $\beta$ -decay measurements as a  $2^+$  state, at 965keV. It is proposed that this is a  $2^+$  member of the  $K=2$ ,  $\gamma$ -band. Its placement in the level scheme can be confirmed using  $\gamma$ - $\gamma$  coincidences in the MINIBALL array.

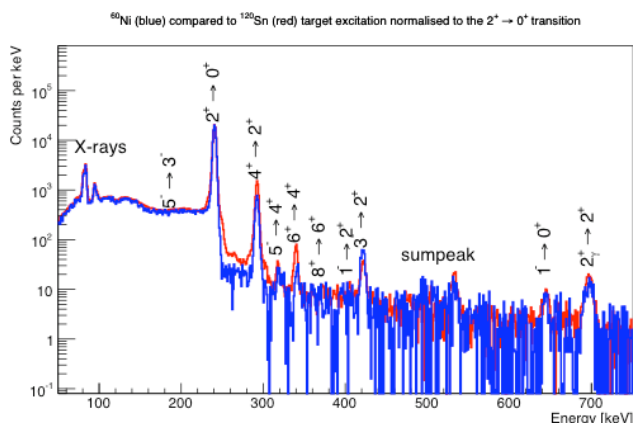


**Figure 1:** MINIBALL spectrum showing de-excitation gamma rays, background subtracted, from  $^{220}\text{Rn}$  after Coulomb excitation with  $^{120}\text{Sn}$  (Blue) and  $^{120}\text{Sn}$  (Red; normalised to  $2^+ \rightarrow 0^+$ ) target at 2.82 A.MeV. One can see how the relative population of the states of interest ( $2^+$ ,  $4^+$ ,  $3^-$ ) changes when varying the mass of the target.

Following this success of using the lighter,  $^{60}\text{Ni}$  target, we ran for 1 extra day with  $^{224}\text{Ra}$  in 2011 on  $^{60}\text{Ni}$ . As with the 2010 campaign, we were able to utilise the "offline" mode of ISOLDE after the protons were no longer impinging on the primary target.

Preliminary analysis using the GOSIA code [3] shows that the collective behaviour of  $^{224}\text{Ra}$  is very similar to that of  $^{226}\text{Ra}$ . A strong E3 matrix element connects the ground state to the first 3- showing enhanced octupole collectivity. Analysis of  $^{220}\text{Rn}$  is still on going, but there is significant population of the negative parity states indicating a strong E3 coupling to the ground state.

References:

- [1] L. P. Gaffney et al., "Contributions to Research at ISOLDE in 2010", (2011) IS475
- [2] H. J. Wollersheim et al., *Nucl. Phys A* **556**, (1993) 261
- [3] T. Czosnyka et al., *Bull. Am. Phys. Soc.* **28**, (1983) 745

L. Gaffney

## IS477: Coulomb Excitation of $^{128}\text{Cd}$

The cadmium isotopic chain remains to be one of the most interesting in modern nuclear structure physics as it is 48 protons and, therefore, two proton holes below the  $Z=50$  shell closure. Coulomb excitation experiments performed at REX-ISOLDE measured for the neutron-rich isotopes  $^{122}\text{Cd}$ ,  $^{124}\text{Cd}$ , and  $^{126}\text{Cd}$  enhanced  $B(E2;0^+ \rightarrow 2_1^+)$ -values [1]. A striking anomaly has been observed for the excitation energy of the first excited  $2^+$ -state in  $^{128}\text{Cd}$  ( $N=80$ ). Contrary to the expectations of a steady increase towards the semi-magic isotope  $^{130}\text{Cd}$ , it is found at a lower energy compared to the corresponding excitation in  $^{126}\text{Cd}$  [Fig.1].

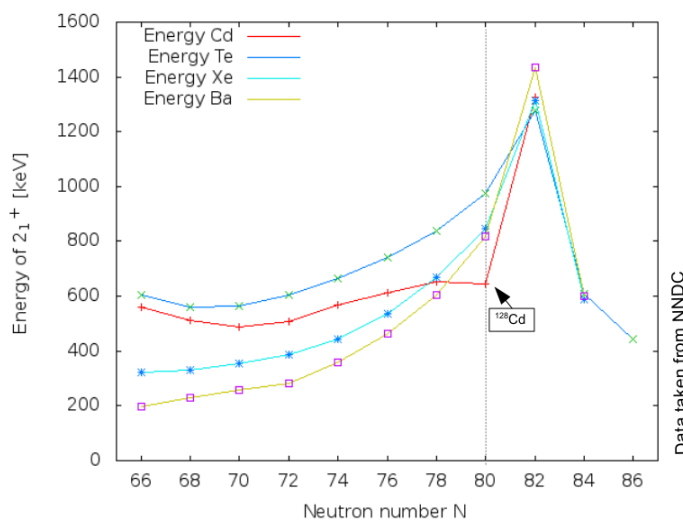


**Fig.1:** Excitation energy of the first  $2^+$ -state for different nuclei.

Currently, only a Beyond Mean Field approach is capable to reproduce these findings [2]. However, these calculations must assume an already considerable prolate deformation. This raises the question about the degree of quadrupole collectivity for this particular nucleus. The relevance of that question is underlined by

the close proximity of this nucleus to the waiting point  $^{130}\text{Cd}$  of the astrophysical r-process which was found to be a typical closed shell nucleus [3]. A measure for the quadrupole collectivity is the  $B(E2; 0^+ \rightarrow 2_1^+)$  reduced transition probability. This quantity is accessible via Coulomb excitation and the extraction of the  $B(E2; 2_1^+ \rightarrow 0^+)$ -value from the excitation probability. Therefore, post-accelerated  $^{128}\text{Cd}$  projectiles are shot on a scattering target. Proportional to the E2-excitation probability the nucleus will exchange a virtual photon with one of the target nuclei resulting in excited nuclei. Obviously, a sufficient number of projectiles, representing a statistically relevant ensemble, are required to measure the cross section of this reaction. ISOLDE represents worldwide the only radioactive beam facility capable to provide this rare isotope in sufficient quantities, so that a post-accelerated beam can be investigated with this versatile experimental tool.

The corresponding experiment on  $^{128}\text{Cd}$  was performed in August 2011 exploiting the outstanding production yield achieved at ISOLDE in combination with the unique capability of a selective ionisation scheme (RILIS) and REX to post-accelerate these rare radioactive ion beams. In the experiment a beam of  $^{128}\text{Cd}$  with an energy of 2.85 MeV/nucleon was delivered to the detection setup. A  $^{64}\text{Zn}$  (1.48 mg/cm<sup>2</sup>) target was used to Coulomb excite the impinging  $^{128}\text{Cd}$  nuclei. Both the scattered projectile and recoiling target nuclei were detected using a double-sided silicon strip detector (DSSSD). The de-excitation  $\gamma$ -rays following the Coulomb excitation were detected by the highly efficient MINIBALL spectrometer consisting of 24 HPGe detectors. Apart from the low intensities, the short half-life of  $^{128}\text{Cd}$  ( $T_{1/2} = 340$  ms) is one of the major challenges. Owing to the time needed for charge-breeding and transport of the isotope of interest from the

primary production to the secondary target, a fraction of the interesting nuclei decays already in flight. This accounts partly for the isobaric beam contaminants, such as  $^{128}\text{In}$  and  $^{128}\text{Sn}$ . Furthermore, the volatile, easily ionized  $^{128}\text{Cs}$  was identified as beam contaminant. The beam composition was disentangled using the  $\Delta E$ -E information obtained with an ionisation chamber and a silicon telescope, as well as the known radioactive decay behaviour. The latter has been recorded in the beam dump and in short runs using a thick  $^{64}\text{Zn}$  stopper target (14.89 mg/cm<sup>2</sup>).

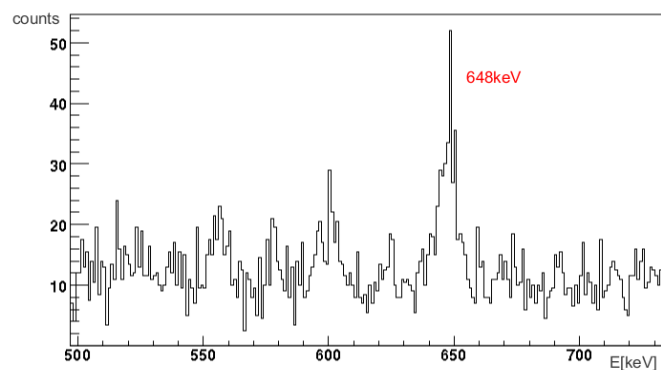


*Fig.2: Doppler-corrected gamma-spectrum with a clear peak at 648 keV stemming from the  $2_1^+ \rightarrow 0^+$  transition in  $^{128}\text{Cd}$ .*

Fig. [2] shows the Coulomb excitation  $\gamma$ -ray spectrum recorded in a total beam time of  $\sim 50$  hours. To create this spectrum a Doppler correction with respect to the beam-like particles and random background subtraction were performed. The 648-keV peak corresponds to the interesting  $2_1^+ \rightarrow 0^+$  transition. With an analysis performed relative to the target excitation (at an energy of 991 keV) and the information about the beam composition as well as the number of  $\gamma$ -rays detected for the 648-keV peak of the  $2_1^+ \rightarrow 0^+$  transition of  $^{128}\text{Cd}$  will allow the extraction of the  $B(E2; 0^+ \rightarrow 2_1^+)$ -value in the ongoing analysis.

References:

- [1] Th. Behrens, *PhD Thesis*, Technische Universität München, 2009  
 [2] T. Rodriguez et al., *Phys. Lett. B* **668**, (2008) 410  
 [3] A. Jungclaus et al., *Phys. Rev. Lett.* **99**, 132501 (2007)

*S. Böinig, Th. Kröll, M. Scheck*

## IS487: Cr<sup>3+</sup> Dynamic off-centering in CdCr<sub>2</sub>S<sub>4</sub> leading to Magnetic-electric Clusters

The cubic spinel CdCr<sub>2</sub>S<sub>4</sub> gained recently a vivid interest, given the relevance of relaxor-like dielectric behavior in its paramagnetic phase. By a singular combination of local probe techniques namely Pair Distribution Function (PDF) and

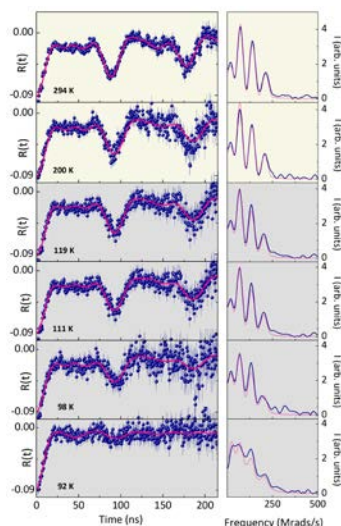


**Figure 1:** Representative  $R(t)$  functions taken at different temperatures.

Perturbed Angular Correlation (PAC) we firmly establish that the Cr ion plays the central key role on this exotic phenomenon, namely through a dynamic off-centering displacement of its coordination sphere. PAC measurements, can infer that the Cr site experiences an ultra-slow dynamics ( $\tau >$

1 ns) in the 119 K – 92 K temperature range while no change is observed in the Cd local environment (see Fig. 1.).

The temperature dependence of lattice parameters,  $[a(T)]$ , obtained from PDFs refinements are depicted in Fig. 2 (top) shows three distinct regimes in the temperature range 80-220 K. For  $T > 130$  K,  $a(T)$  displays a conventional linear contraction on cooling. A change of this monotonic trend occurs at  $T_F \sim 130$  K where an expansion regime sets in. The temperature dependence of the amplitude of the off-centering displacements ( $\Delta r$ ) is displayed in Fig. 2 (bottom) where a maximum value of 0.011 Å was obtained.

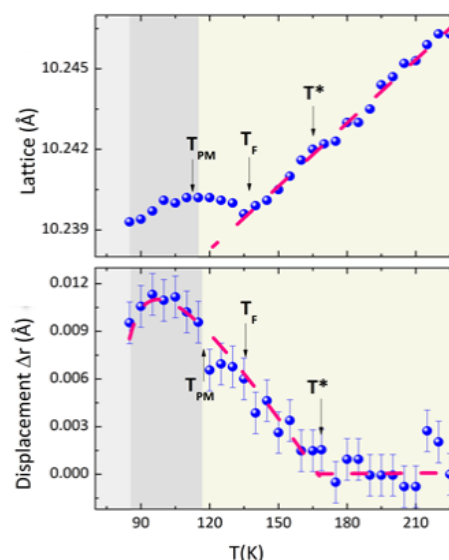


**Figure 2:** Temperature dependence lattice parameters (top). Amplitude of the Cr local off-centering (bottom).

We further show that this off-centering of the magnetic Cr-ion gives rise to a peculiar entanglement between the polar and magnetic degrees of freedom, stabilizing, in the paramagnetic phase, short range magnetic clusters, clearly seen in ultra-low field susceptibility measurements in the form of step-like behaviour in temperature range between the ordering temperature  $T_C \sim 86$  K and  $T_{PM} \sim 116$  K. This feature in the paramagnetic (PM) regime is a

fingerprint of the presence of short-range magnetic clusters (see Fig. 3 left). Landau theory demonstrates the role of a linear coupling between the magnetic and polar order parameters on the appearance of magnetic cluster in paramagnetic phase of this compound (see Fig. 3 right).

This new discovery and interpretation open insights on the hotly debated magnetic and polar interaction, setting a step forward in the reinterpretation of the coupling of different physical degrees of freedom.

In summary, our PDF, PAC and M(T) experimental findings prove the existence of a dynamic state caused by the presence of simultaneous polar and magnetic nanoclusters, pointing to the birelaxor nature of the system. Our results are consistent with a picture where the effects described in the recent literature arise from Cr<sup>3+</sup>-atomic displacements occurring well above the magnetic ordering temperature.

Our combined analysis clearly shows that the increasing of the average size of random oriented dipoles or polar nanoclusters saturates at TPM, concomitantly with the onsets of their dynamic slowing down and Cr<sup>3+</sup>-Cr<sup>3+</sup> magnetic correlations. We also show that an ultra slow Cr<sup>3+</sup>

transition pointing to its order-disorder type origin.

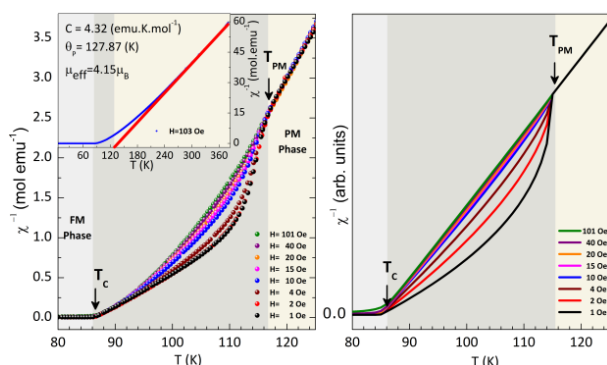


**Figure 3:** *left:*  $\chi^{-1}(T)$  with different applied magnetic fields 1-101 Oe; *Inset:*

$\chi^{-1}(T)$  measured on heating and with  $H = 103$  Oe. *right:*  $\chi^{-1}(T)$  resulting from theoretical calculations of the phase transitions Landau theory, considering linear magneto-electric coupling.

We speculate that this Cr<sup>3+</sup> dynamic off-centering is intrinsically entangled to the formation of local dipoles, which are responsible for the observed magnetic correlations between adjacent Cr<sup>3+</sup> neighbours. We further confirm this electric and magnetic orders entanglement by modeling the peculiar low-field  $\chi^{-1}(T)$  measurements via Landau theory using a linear magneto-electric coupling.

*G. Oliveira*

## IS489: New online diffusion setup comes to ISOLDE

The application of radioactivity in solid state physics dates back to the early days of nuclear physics. The first such application of "tracer methods" was by van Hevesy in the early 1920s to investigate self-diffusion in Pb [1]. Studying diffusion in solids by exploiting radioactive isotopes remains one of the most efficient means of exploring diffusion processes with high sensitivity, in particular allowing the ability to study self-diffusion in a relatively straightforward way. Furthermore, the possibilities of exploring diffusion processes using radioactivity are greatly enhanced when coupled to an isotope factory such as ISOLDE.

The principles behind radiotracer diffusion have remained essentially unchanged since the earliest experiments: radioactivity is introduced into a sample – in the case of ISOLDE via implantation – then thermal treatments allow the radioactive isotopes to diffuse into the material. The sample is then "sliced" – usually using a polishing apparatus – and, by measuring the activity

of the resulting slices, allows a diffusion profile to be determined. A very active programme exploring diffusion has already been underway at ISOLDE for many years and in recent times has focussed on the anomalous diffusion profiles seen in compound semiconductors such as CdTe[2,3]. A limitation of the technique until now has been that half-lives of about 1 hour and below have been out of experimental reach. This has meant that some highly interesting cases such as magnetic dopants in semiconductors and long-standing questions such as self-diffusion in Al have been tantalisingly excluded from the experimental programme.

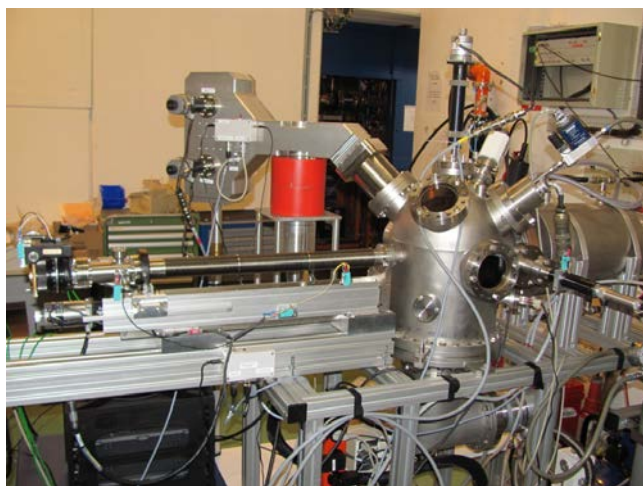


**Figure 2** Installation of the new online diffusion chamber at ISOLDE in 2011.

However, in summer 2011, an online diffusion chamber which will allow these isotopes – among others – to be finally studied was delivered to ISOLDE and installed and tested at LA1. This chamber incorporates all the basic elements of a traditional radio-tracer apparatus as described above, but every step will be carried out *in situ*, without breaking the vacuum. The sample will be implanted using the ISOLDE beam; thermal treatments (up to 1600 °C) to trigger the diffusion will be carried out by transporting the sample into

the on-board furnace; sectioning of the sample is achieved using an Ar<sup>+</sup> ion gun and a tape station catches the sputtered activity and transports it to a Ge detector where the gamma spectrum will be measured. The initial tests at LA1 in 2011 were promising and the chamber will now be semi-permanently installed at the GLM beam line in early 2012, where “parasitic” collections will be possible in addition to the well-defined programme of IS489. The combination of ISOLDE – with its range of beams – and this unique chamber should make for a very exciting physics run in 2012.

#### References:

- [1] J. Gróh and G. v. Hevesy, *Ann. Phys.*, 65, 216 (1921).
- [2] H. Wolf, F. Wagner, Th. Wichert, and ISOLDE Collaboration, *Phys. Rev. Lett.* 94, 25901 (2005).
- [3] H. Wolf, J. Kronenberg, F. Wagner, Th. Wichert, and Isolde Collaboration, *Pre-requisites for the formation of unusual diffusion profiles in II-VI semiconductors*, *Phys. Status Solidi B* 247, 1405 (2010).

*K. Johnston*

### **IS496: First measurement of the $B(E2; 2^+_1 \rightarrow 0^+_1)$ value of $^{140}\text{Nd}$**

From July 1<sup>st</sup> to July 4<sup>th</sup>, 2011, the first part of experiment IS496 was performed with the Coulomb excitation of radioactive, proton-rich  $^{140}\text{Nd}$  nuclei at MINIBALL. The final goal of the full IS496 experiment is the study of the effect of shell stabilization of the collective isovector valence-shell excitations along the N=80 isotonic chain [1,2]. As a first step the  $B(E2)$  value of the first excited  $2^+$  state of  $^{140}\text{Nd}$  was measured, which is essential for the interpretation of further data, to be taken in

2012 for  $^{142}\text{Sm}$  and in 2014/2015 at HIE-ISOLDE for both isotopes, where also the investigation of higher-lying (mixed-symmetry) states is foreseen.

The RILIS ion source and its newly developed ionization scheme for Neodymium was used in combined laser-on/laser-off runs in order to estimate the fraction of  $^{140}\text{Nd}$  ions in the beam besides the main contaminant  $^{140}\text{Sm}$ . Data was taken for almost 60 hours at an average current of 1-2 pA. Two different targets,  $^{48}\text{Ti}$  and  $^{64}\text{Zn}$ , were used for projectile-Coulomb excitation reactions. The beam energy was constant at 2.85 MeV/u. Figure 1 shows the random-background subtracted Coulomb-excitation spectra, Doppler-corrected for beam particles with  $A=140$  as well as for target excitation. The gamma-ray spectra are dominated by the decays of the first  $2^+$  states of  $^{140}\text{Sm}$ ,  $^{140}\text{Nd}$  and  $^{48}\text{Ti}$ , respectively. The Coulomb excitation cross-section of  $^{140}\text{Nd}$  has been normalized to the excitations of the targets. A conclusive analysis with the multi-step Coulomb-excitation code GOSIA [3] uses various ranges of scattering angles, covered by the CD-shaped particle detector. The preliminary result for the  $B(E2; 2^+_1 \rightarrow 0^+_1)$  value of  $^{140}\text{Nd}$  is **30(5) W.u.** representing first information on that quantity.

This value is larger than expected from QPM calculations for  $N=80$  isotones, that yield 17 W.u. [4], only. The calculations need to be modified in order to describe the new data while simultaneously keeping the satisfactory description of the Ce, Ba, and Xe isotones [5].

A more detailed analysis is ongoing and especially the extraction of the  $B(E2)$  value of the contaminant  $^{140}\text{Sm}$  seems to be an exciting possibility.

References:

- [1] N. Pietralla et al., INTC P-268 (2009)  
 [2] G. Rainovski et al., Phys. Rev. Lett. 96,

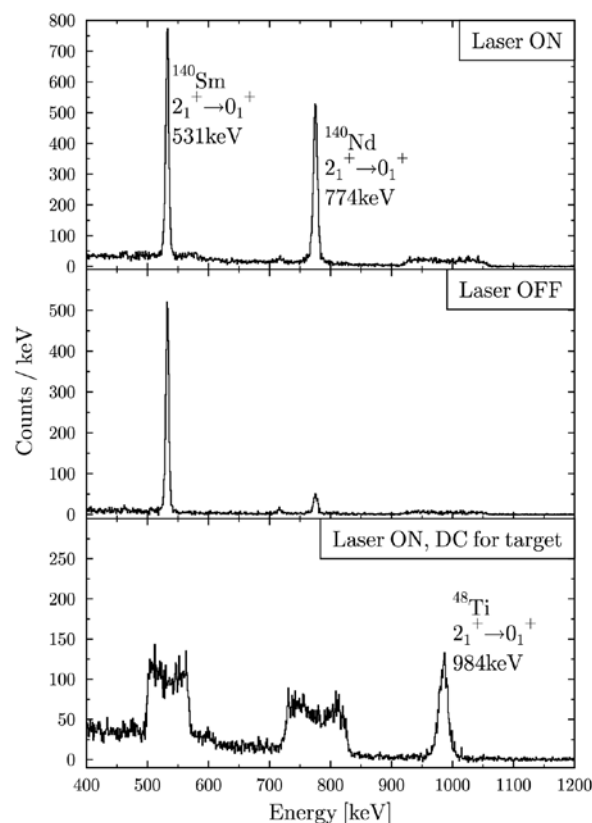


**Figure 3:** Doppler-corrected  $\gamma$ -ray spectra after subtraction of random background. The Doppler correction was done with respect to the projectile (top, middle) or target nuclei (bottom). The laser ionization was used for the top and bottom spectra.

122501 (2006)

[3] T. Czosnyka et al., Bull. Am. Phys. Soc. 28, 745 (1983)

[4] Ch. Stoyanov, private communication

[5] N. Lo. Iudice et al., Phys. Rec. C 77, 044310 (2008)

*C. Bauer*

## IS492: Recent results from radiotracer PL at ISOLDE

Photoluminescence (PL) spectroscopy is one of the most commonly used techniques in the characterization of semiconductors, enabling high resolution study of even low

concentrations of defects in the material relatively easily. However, one of the main limitations of the technique is its chemical blindness, and so identifying the origin of features can take many years – even decades. The combination of PL with radioactive isotopes offers the possibility to gain that otherwise-lacking chemical dimension. Furthermore, by combining techniques such as uniaxial stress and Zeeman spectroscopy with PL we are able to gain structural and electronic information about the centres, allowing a very complete description and understanding of PL systems.

PL has been carried out at ISOLDE since the mid-1990s, and now includes an on-site off-line laboratory for the study of the effects of relatively short-lived isotopes. Recent focus has been on identifying impurities in ZnO and on unraveling what were thought to be well-understood systems in Si.

#### (a) Donor-related impurities in ZnO

After a burst of activity in the 1960s, the study of ZnO remained something of a niche area until the early 2000s when predictions such as room temperature ferromagnetism and the demand for blue/UV laser emissions drove researchers to “re-discover” this material once again. However, in spite of considerable effort, many of the fundamental properties of the material remained unclear: although well-known to be an n-type semiconductor many of the impurities giving rise to this behaviour remained unidentified. Work carried out at ISOLDE has helped to identify a number of the donor defects responsible for this behaviour and has also opened up some new avenues of research exploring the roles of double donors and isoelectronic impurities in the material.

Figure one shows a snapshot from the periodic table in and around Zn. The group III elements Al, Ga and In – when occupying a Zn site in ZnO – become single

donor impurities, and the range of beams available at ISOLDE allowed implantations of Zn, Ga, In, Cd, Ag and As to be carried out to investigate the behaviour of donor impurities in ZnO. These experiments have provided the first chemical identification that Ga and In are responsible for at least four of the ten main optical features commonly seen in this material. Furthermore, luminescence has been observed for Ge impurities for the first time, and recent work has focused on the performing Zeeman and stress experiments on Ge-centres and also on isoelectronic impurities such as Hg and Cd.

#### Recent publications involving ZnO

i. Karl Johnston, Joseph Cullen, Martin Henry, Enda McGlynn and Monica Stachura “Evidence for As lattice location and Ge bound exciton luminescence in ZnO implanted with  $^{73}\text{As}$  and  $^{73}\text{Ga}$ ” Physical Review B 83 125205 (2011).

ii. J. Cullen, K. Johnston, M. O. Henry, E. McGlynn and the ISOLDE Collaboration “Photoluminescence due to group IV impurities in ZnO” Accepted for publication in MRS proceedings” (2012)

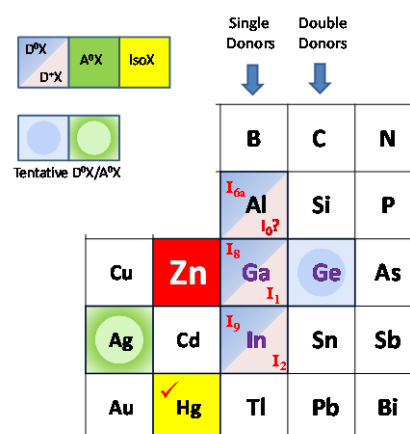


**Figure 1:** Elements to the right of Zn will act as donors in ZnO, if occupying a Zn site. Experiments at ISODLE have allowed the chemical identification of PL features

associated with Ga, In and Ge in ZnO for the first time.

### (b) Metal impurities in mono-isotopic Si

Silicon is still far and away the pre-eminent semiconductor and lays strong claims to be the most studied material in the world. Its extensive use in the electronics industry and increasing deployment as the basis for solar cells demands a detailed understanding of the role of defects in this material. However, although a great deal is known about defects and impurities in Si, surprises can still occur. In the past few years very pure essentially mono-isotopic  $^{28}\text{Si}$  has been produced – a by-product from the Avogadro project: an initiative to re-define the kg in terms of Avogadro's constant. When studied using PL the spectra were quite unlike any others previously seen in Si. In particular, the spectral features were much sharper than for natural Si due to the elimination of inhomogeneous isotope broadening. This drastic narrowing of features can be seen in figure 2(a) where the original optical line is shown to consist of a forest of separate lines.

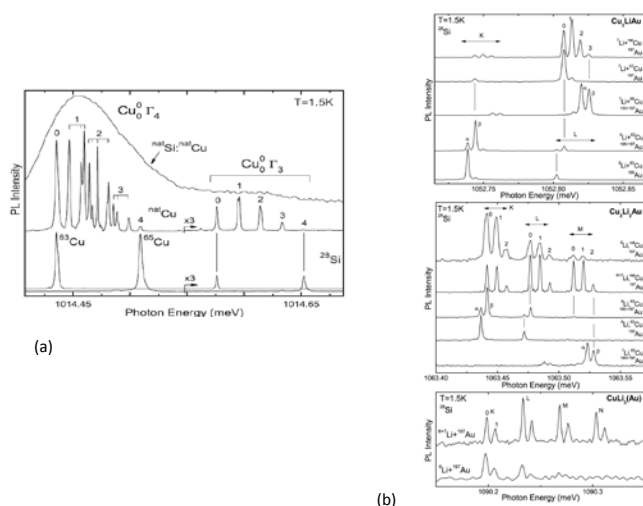


**Figure 2** Example of PL spectra obtained from  $^{28}\text{Si}$ . (a) shows the narrowing of optical features which takes place in one Cu-related centre. (b) shows spectra obtained after implantation at ISOLDE from a  $^{197}\text{Au}$  beam.

These individual features can be understood in terms of the number of atoms involved in the centre and further study into this area produced more surprises; it turns out that many of the previously studied centres which were thought to originate from isolated or pairs of transition metals actually turn out to be multi-atom centres e.g. four Cu atoms. The  $\text{Cu}_4$  centre can be thought of as a base, and this can then in turn be “decorated” with other metals such as Ag or Li, or with Li or Ag replacing a Cu atom in the complex. Determining the numbers of atoms in the centres requires at least two isotopes of the same element, and uniquely, ISOLDE work has combined enriched silicon material with radioactive isotopes in the case of Au impurities for which there is only one stable isotope. Implantations at ISOLDE of  $^{197}\text{Au}$  – produced from a  $^{197}\text{Hg}$  beam, and decaying into  $^{197}\text{Pt}$  – allowed these studies to be furthered and resulted in the observation of several new Au- and Pt-related multi-atom centres involving Cu in Si.

There is great excitement in the semiconductor community about these results, and not just in the ‘Ivory Towers’. Centres involving transition metals have a significant effect on device performance, especially on the efficiency of solar cells. The radically different picture of impurities in Si offered by these experiments may allow a greater understanding of impurities in Si leading ultimately to more efficient and reliable devices.

### Recent Publications involving Si

i. M. Steger, A. Yang, T. Sekiguchi, K. Saedi, M. L. W. Thewalt, M. O. Henry, K. Johnston, H. Riemann, N. V. Abrosimov, M. F. Churbanov, A. V. Gusev, A. K. Kaliteevskii, O. N. Godisov, P. Becker, H.-J. Pohl “Photoluminescence of deep defects involving transition metals in Si – new

insights from highly enriched  $^{28}\text{Si}$ " Applied Physics Reviews 110 081301 (2011)

ii. M. Steger, A. Yang, T. Sekiguchi, K. Saeedi, M. L. W. Thewalt, M. O. Henry, K. Johnston, E. Alves, U. Wahl, H. Riemann, N. V. Abrosimov, M. F. Churbanov, A. V. Gusev, A. K. Kaliteevskii, O. N. Godisov, P. Becker, and H.-J. Pohl "Isotopic fingerprints of Pt containing luminescence centers in highly enriched  $^{28}\text{Si}$ " Physical Review B 81 235217 (2010)

iii. M. Steger, A. Yang, T. Sekiguchi, K. Saeedi, M.L.W. Thewalt, M.O. Henry, K. Johnston, H. Riemann, N.V. Abrosimov, M.F. Churbanov, A.V. Gusev, A.D. Bulanov, I.D. Kaliteevski, O.N. Godisov, P. Becker, H.-J. Pohl "Isotopic fingerprints of gold-containing luminescence centers in  $^{28}\text{Si}$ " Physica B 404 5050 (2009)

*K. Johnston, M. Henry*

## IS497: Ground States and Isomers of Cadmium by High-Resolution Laser Spectroscopy

The isotopic chain of cadmium was studied by high-resolution laser spectroscopy for the first time. The goal was to determine nuclear spins, electromagnetic moments and root mean square (rms) charge radii of ground and isomeric states along the isotopic chain, ultimately reaching the neutron 50 and 82 shell closures.

In 2011 the intense beams of  $^{106-124,126}\text{Cd}$  were studied by fluorescence spectroscopy, which also covered the isomers in the odd  $^{111-123}\text{Cd}$ . The measurements were carried out with the collinear laser spectroscopy setup at ISOLDE-CERN. High-energy protons impinging on a uranium carbide target produced neutron-rich cadmium isotopes, which were laser ionized, accelerated to energy of 50keV and mass separated with the general purpose

separator (GPS). The beam was neutralized in a sodium cell. The cadmium atoms were then excited in the transition  $5s5p\ ^3P_2 \rightarrow 5s6s\ ^3S_1$  at a wavelength of 509 nm. Laser excitations in the components of the hyperfine structure (hfs) were identified by the beam fluorescence as a function of the Doppler-shifted laser frequency while scanning the beam velocity. A typical spectrum of  $^{115}\text{Cd}$  is presented in Fig. 1, where one can identify the hfs components of the ground state and the isomer.

The measurements determined the ground-state spins in the studied range as being 1/2, 3/2, and 5/2 in close relation with the corresponding single-particle orbitals of the *sdgh* shell. Evidence is found whether the isomeric configuration is 11/2<sup>-</sup> in all odd cases. The data is sensitive to the changes in the degree of collectivity between the ground states and the isomers, not only from their quadrupole moments, but also through their rms charge radii. This has the potential to solve the question if the cadmium isotopes are spherical vibrators or weakly deformed rotors.

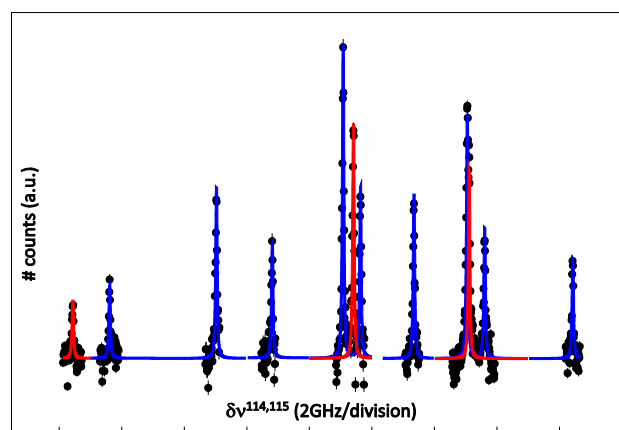


**Figure 4** Hyperfine structure of  $^{115}\text{Cd}$  (red) and  $^{115}\text{Cd}^m$  (blue).

It is planned to extend the measurements towards the neutron 50 and 82 shell closures in 2012 to address isotopes of specific interest in these regions. In order to improve the sensitivity to the very exotic

species at both ends of the shell, the measurements will be carried out using bunched beams from ISCOOL. Furthermore, the  $5s\ 2S_{1/2} \rightarrow 5p\ 2P_{3/2}$  transition at 215 nm in the cadmium ion will be used. Offline tests have shown the feasibility of the experiment.

*D.T. Yordanov for the COLLAPS Collaboration*

## IS501: Lattice locations and properties of Fe in Co/Fe co-implanted ZnO

Magnetic semiconductors obtained by dilute doping with 3d-metal impurities have been of major interest in recent years due to the potential applications in spintronics. For ZnO, room-temperature ferromagnetism was predicted by theory [1], but grossly inconsistent experimental results have been obtained.

At ISOLDE, our group, utilizing  $^{57}\text{Fe}$  emission Mössbauer spectroscopy following implantation of the parent  $^{57}\text{Mn}$  ( $T_{1/2} = 1.5$  min.), has been investigating the role of Fe in ZnO. Our results have shown that in the dilute regime ( $<10^{13}$   $^{57}\text{Mn}/\text{cm}^2$ ), the Fe is found as  $\text{Fe}^{2+}$  and  $\text{Fe}^{3+}$  in paramagnetic sites, and spectra shows the absence of any spin interactions with defects created in the implantation process [2] i.e. suggesting that dilute Fe impurities cannot be the source of magnetism observed by some authors.

Moreover, Mössbauer spectra obtained from conversion electron Mössbauer spectroscopy (CEMS) on samples implanted with  $>10^{15}$   $^{57}\text{Fe}/\text{cm}^2$  are very different from those obtained by us using  $^{57}\text{Mn}$ . To elucidate this apparent dilemma, a sample was implanted with  $^{57}\text{Co} \sim 5 \times 10^{12}$   $\text{cm}^{-2}$  with an impurity level of  $^{57}\text{Fe}$  of  $\sim 5 \times 10^{14}$   $\text{cm}^{-2}$ . Although for most cases an unacceptable level of contamination, this was beneficial for the current study, bridging the gap

between ISOLDE experiments with  $^{57}\text{Mn}$  and home laboratory studies using  $^{57}\text{Fe}$ . Some of the spectra obtained are shown in Fig. 1.

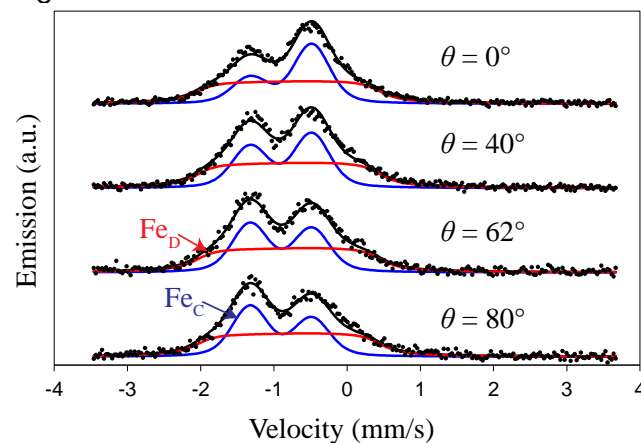


*Fig. 1:  $^{57}\text{Fe}$  emission Mössbauer spectra obtained of an Fe/Co implanted sample at room temperature under the emission angles relative to the crystal symmetry axis as indicated (from [3]).*

One conclusion is evident from the spectra in Fig. 1; the spectra clearly depend on the emission angle. This shows that some of the probe atoms are in an environment where they can “see” the lattice structure, or in crystalline sites ( $\text{Fe}_C$ ). Another part of the probe atoms are in an environment, not showing any angular dependence ( $\text{Fe}_D$ ), most likely in a damage environment, where information on the local lattice structure is lost. Both fractions are due to  $\text{Fe}^{2+}$ . Although the splitting of the two lines of the crystalline component ( $\text{Fe}_C$ ) is higher than is observed for  $\text{Fe}^{2+}$  substituting  $\text{Zn}^{2+}$  in ZnO, the electron density is exactly the same, and the increased splitting is probably due to small distortions of the lattice. The spectra obtained by us are practically identical to spectra obtained by CEMS on  $^{57}\text{Fe}$  implanted samples. However, angular dependence was not considered in those measurements.

From low temperature measurements [3], it was observed that the relative spectral fraction of the damage fraction component

(Fe<sub>D</sub>) became much higher than that of the crystalline fraction (Fe<sub>C</sub>). This is well known from Mössbauer spectroscopy, if the Debye-Waller factor of the fraction that increases relatively in intensity at lower temperatures is much lower than that of the crystalline site. This is characteristic for an interstitial type of defect, where there is less binding to the lattice.

Upon annealing at  $T > 400^\circ\text{C}$  part of the damage iron component (Fe<sub>D</sub>) was found to be relocated into Fe<sup>3+</sup> species showing fast spin relaxation. The most likely cause of this spin relaxation is spin-spin relaxation between close ( $<5 \text{ \AA}$ ) Fe<sup>3+</sup> pairs: evidence of the first stages of precipitation. Such precipitates would easily give a signal in magnetic measurements and these findings show a possible pathway for the formation of such precipitates [3].

References:

[1] T. Dietl, H. Ohno, F. Matsukura, J. Cibert, and D. Ferrand, Zener Model Description of Ferromagnetism in Zinc-Blende Magnetic Semiconductors, *Science* **287** (2000) 1019

[2] H. P. Gunnlaugsson, T. E. Mølholt, R. Mantovan, H. Masenda, D. Naidoo, W. B. Dlamini, R. Sielemann, K. Bharuth-Ram, G. Weyer, K. Johnston, G. Langouche S. Ólafsson, H. P. Gíslason, Y. Kobayashi, Y. Yoshida, M. Fanciulli and the ISOLDE Collaboration, Paramagnetism in Mn/Fe implanted ZnO, *Appl. Phys. Lett.* **97** (2010) 142501, doi:10.1063/1.3490708

[3] H. P. Gunnlaugsson, K. Johnston, T. E. Mølholt, G. Weyer, R. Mantovan, H. Masenda, D. Naidoo, S. Ólafsson, K. Bharuth-Ram, H. P. Gíslason, G. Langouche, M. B. Madsen and the ISOLDE Collaboration, Lattice locations and properties of Fe in Co/Fe co-implanted ZnO, *Appl. Phys. Lett.* **100** (2012) 042109, doi: 10.1063/1.3679692

*H. Gunnlaugsson for the Mössbauer collaboration at ISOLDE/CERN*

## IS504: Probing the semi-magicity of <sup>68</sup>Ni via the <sup>3</sup>H(<sup>66</sup>Ni, <sup>68</sup>Ni)p two-neutron transfer reaction in inverse kinematics

The region around the nucleus <sup>68</sup>Ni, with a shell closure at  $Z = 28$  and a sub-shell closure at  $N = 40$ , has drawn considerable interest over the past decades. <sup>68</sup>Ni has properties that are typical for a doubly-magic nucleus, such as a high excitation energy and low  $B(E2:2^+-0^+)$  transition probability for the first excited  $2^+$  level [1-3] and a  $0^+$  level as the first excited state [4]. However, recently it has been suggested that the magic properties of <sup>68</sup>Ni arise due to the fact that the  $N = 40$  separates the negative parity pf shell from the positive parity  $1g_{9/2}$  orbital [5,6], and indeed, recent mass measurements [7,8] have not revealed a clear  $N = 40$  shell gap. Despite all additional information that was acquired over the last decade the specific role of the  $N = 40$  is not yet understood and a new experimental approach to study <sup>68</sup>Ni was proposed. Namely, a two neutron transfer (t,p)-reaction on <sup>66</sup>Ni to populate amongst others the  $0^+$  ground state and characterize the  $0^+$  and  $2^+$  excited states in <sup>68</sup>Ni. The nature of low lying  $0^+$  states in <sup>68</sup>Ni have recently been discussed in [9].

The experiment was successfully performed in September 2011. A <sup>66</sup>Ni beam with an average intensity of  $4.2 \times 10^6$  pps was accelerated to an energy of 2.6 MeV/u using REX and directed onto a tritium loaded titanium target in the T-REX particle detection array [10].  $\gamma$  rays were detected using MINIBALL. The beam energy was reduced to avoid fusion with titanium in the target. The target ladder was put at a high voltage (+2000V) to avoid that electrons would reach the silicon detectors of the CD and Barrel in T-REX.

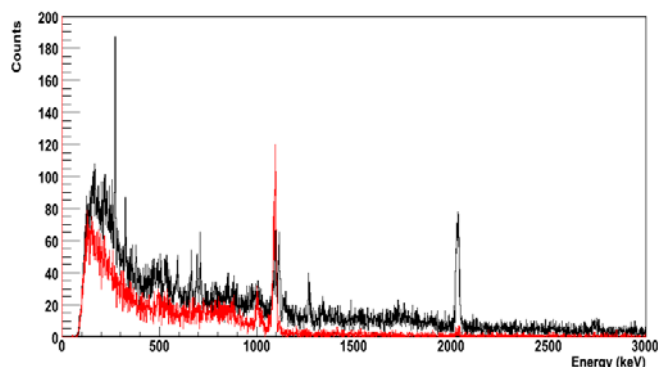


**Figure 1:** Doppler-corrected gamma rays in coincidence with protons. The black spectrum shows prompt coincidences and the red random coincidences.

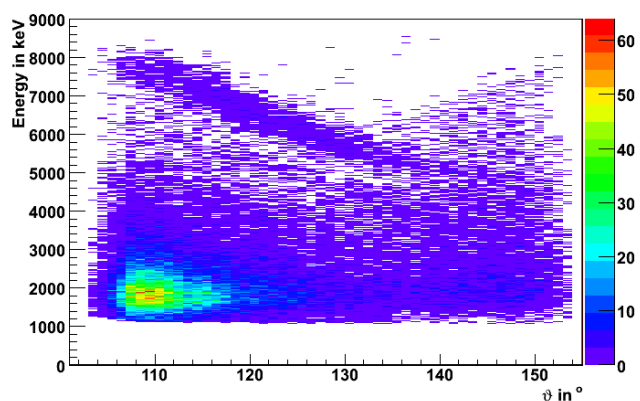


**Figure 2:** Proton energy versus laboratory scattering angle. Transfer to the ground state is clearly present.

A first analysis of the data at IKS, KULeuven indicates the population of several states in  $^{68}\text{Ni}$ . Figure 1 shows the Doppler-corrected  $\gamma$  rays that were observed with MINIBALL in coincidence with protons. The black spectrum shows prompt coincidences and the red spectrum the random coincidences. The preliminary analysis shows a surprising result, namely, except for the ground state, which has a strong population (see Figure 2), we do not see clear evidence for the population of other  $0^+$  states through the two-neutron transfer.

References:

[1] R. Broda et al., Phys. Rev. Lett. 74, 868 (1995).

[2] O. Sorlin et al., Phys. Rev. Lett. 88, 092501 (2002).

[3] N. Bree et al., Phys. Rev. C 78, 047301 (2008).

[4] M. Bernas et al., Phys. Lett. B 113, 279 (1982).

[5] H. Grawe and M. Lewitowicz, Nucl. Phys. A 693, 116 (2001).

[6] K. Langanke et al., Phys. Rev. C 67, 044314 (2003).

[7] S. Rahaman et al., Eur. Phys. J. A 34, 5 (2007).

[8] C. Guénaut et al., Phys. Rev. C 75, 044303 (2007).

[9] D. Pauwels et al., Phys. Rev. C 82, 027304 (2010).

[10] V. Bildstein et al., Prog. Part. Nucl. Phys. 59, 386 (2007).

*J. Elseviers on behalf of the IS504 collaboration*

## IS518: New mass values of neutron-rich Fr and Ra from ISOLTRAP

The masses of very neutron-rich francium and radium isotopes,  $^{224,226,228-233}\text{Fr}$  and  $^{233,234}\text{Ra}$ , have been determined at ISOLTRAP [1] in 2011. The results include six masses:  $^{228,231-233}\text{Fr}$  and  $^{233,234}\text{Ra}$ , which have been measured for the first time. The other mass values have been improved.

The ISOLTRAP measurement cycle starts with accumulation, cooling and bunching of the ISOLDE beam in a radio-frequency quadrupole (RFQ) buncher. From there, the ions are transferred to the recently implemented electrostatic ion-beam trap (MR-ToF-MS [2,3]; see also ISOLDE-newsletter 04/2011). Together with a fast-switching beam-gate it serves as a multi-reflection time-of-flight mass separator. In a second purification step, the ions of interest

are exposed to a mass-selective buffer-gas cooling technique in a preparation Penning trap. Finally, the actual mass measurements are performed in the precision Penning trap. The ISOLTRAP setup is sketched in Fig. 1. Although nuclei around magic numbers have been subject to extensive studies, not much data exists for the evolution of the  $N=126$  shell. The new data provide two-neutron separation energies  $S_{2n}$  up to  $N=146$  thus offering information about structural changes even towards the next shell closure at  $N=168$ . Furthermore, they serve as valuable input for the development of nuclear structure models in this very heavy, neutron-rich mass region. In addition, these masses lie in a region particularly interesting for nucleosynthesis [4] since the rapid neutron-capture process ( $r$ -process) can recycle due to the process of fission. Together with the Rn data from 2008 [5], the Fr and Ra masses provide beta-decay energies for the evaluation of beta-decay half-lives that greatly influence the  $r$ -process. Thus, the new mass values can help to consolidate the nucleosynthesis path for the  $r$ -process.

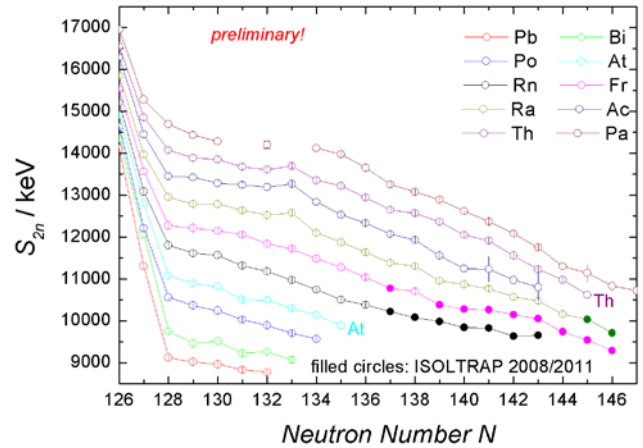


**Figure 2:** Two-neutron separation energies of Ra, Fr, and Rn isotopes including the new values based on the recent ISOLTRAP measurements.

References:

- [1] M. Mukherjee et al., Eur. Phys. J. A 35 (2008) 1.
- [2] R. N. Wolf et al., Hyperfine Interact. 199 (2011) 115.
- [3] R. N. Wolf et al., Int. J. Mass Spectrom. 313 (2012) 8.
- [4] D. Lunney et al., Rev. Mod. Phys. 75 (2003) 1021.
- [5] D. Neidherr et al., Phys. Rev. Lett. 102, 112501 (2009)

*M. Rosenbusch for the ISOLTRAP collaboration*

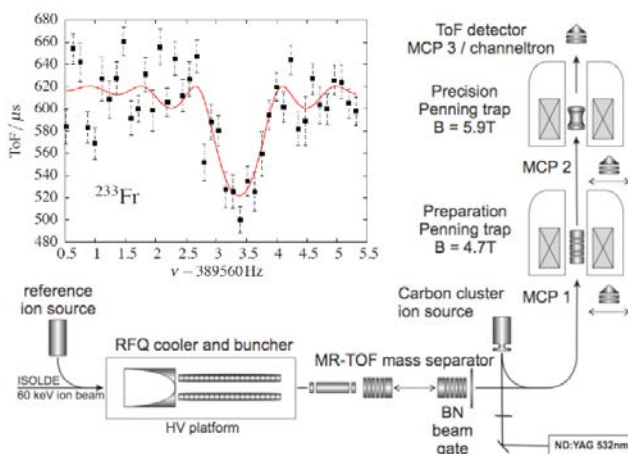


**Figure 1:** Sketch of the ISOLTRAP mass spectrometer with its linear Paul trap, electrostatic ion-beam trap, and two Penning traps. Upper left: time-of-flight resonance of the recently measured  $^{233}\text{Fr}$ .

## Target and Ion Source Development:

The program on target and ion source development resulted last year in different beam improvements and new technologies used for the first time in an "online" configuration. This combines online operation of ion sources, such as a cold plasma Helicon ion source, a bulk Rhenium surface ion source and a VADIS ion source mounted on a molten lead target unit, a RF-driven LIST trap combined with RILIS for the purification of beams, new types of targets such as calcium oxide nanomaterials displaying improved release properties, and last but not least, a molten fluoride salt target under development for neutrino physics. Figure 1 provides an overview of these different results.

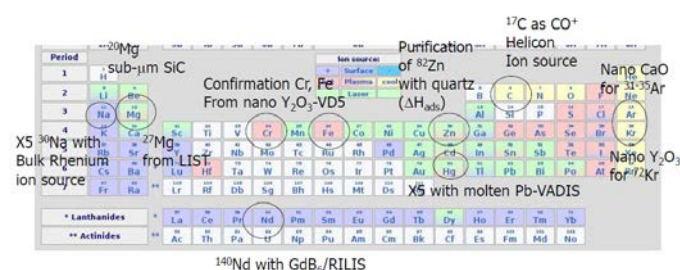


**Figure 1:** Highlights on delivered beams and developments which took place in 2011 at ISOLDE.

Following up on the report given in the previous Newsletter, year 2011 witnessed first in-beam tests of a Helicon-type cold plasma ion source developed by Pekka Suominen for the production of molecular neutron-rich carbon beams [1]. With IS445, stable operation and delivery of  $^{16,17}\text{C}$  as  $\text{CO}^+$  ions could be monitored, with yet too low intensities to fulfill their physics objectives. The two stage extraction electrode configuration provided adequate online beam profiles, Figure 2.



**Figure 2:** Helicon source seen from the beam extraction side, with the visible first extraction stage.

This project is now taken over by Dr Matthias Kronberger, previously active in  $\text{H}^+$  ion source development for the injector upgrades under construction at CERN, hoping we can find an additional margin for efficiency improvements. Another milestone was the successful operation of the LIST technology, jointly developed within a collaboration of the TISD, the RILIS and Mainz university teams [2]. When combined with a Titanium foil target, suppression factors of isobaric impurities of more than 3 orders of magnitude could be achieved, whereas RILIS Mg ions could be delivered with some x30 yield drop on average. After these successful online tests, further developments are taking place together with a foreseen first unit to deliver beam to physics experiments this year. These different developments were completed with the confirmation that a VADIS ion source is suitable to produce intense and pure mercury beams from a molten lead target, leading to a fivefold improvement on intensities versus the ones obtained with historical MK3 FEBIAD ion sources, Figure 3. Full compatibility of the VADIS molybdenum cavity with metal vapors and no pollution of the extraction electrode could be confirmed. Finally amongst the developments that took place on the ion source technologies, a bulk rhenium cavity was designed and manufactured to replace the more

traditional surface ion sources made of tungsten, tantalum or niobium. With its high work function of ca 5eV, improvements on ionization efficiencies, hence of  $^{30}\text{Na}$  beam intensities, were witnessed, and will also hopefully serve for some future requests on alkali and earth-alkali elements.

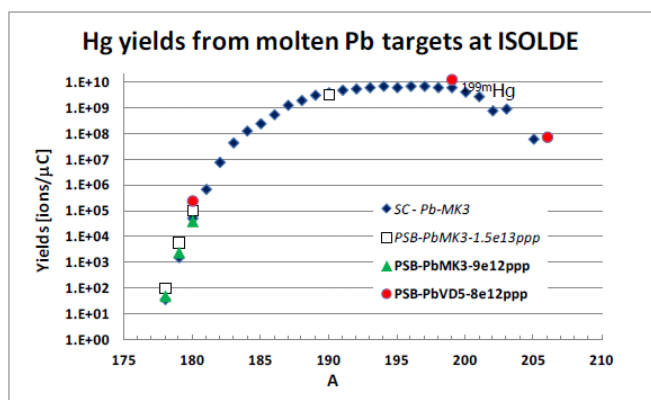


**Figure 3:** Comparison of yields of mercury beams from molten lead targets.

On the front of target material developments, highlights were obtained last year by the extension of the ISOLDE nanomaterials portfolio with a third member in the family, calcium oxide joining up the available silicium carbide and yttrium oxide materials, Figure 4. This result, which already provided the WITCH experiment with high yields of  $^{35}\text{Ar}$  beams, is even more interesting for more exotic beams, for which reduced diffusion times that originate from the nanostructure translates into increased yields. The conservative operation temperatures and proton pulse intensities allowed us to provide beams with constant intensity over several days, quite on the contrary to what was observed with previous CaO targets operated at ISOLDE at higher temperatures and higher proton pulse intensities. This work was the subject of a master thesis in material sciences by Joao Pedro Ramos, for which he obtained

19/20, equivalent to the highest honors for such a diploma at the University of Aveiro [3].

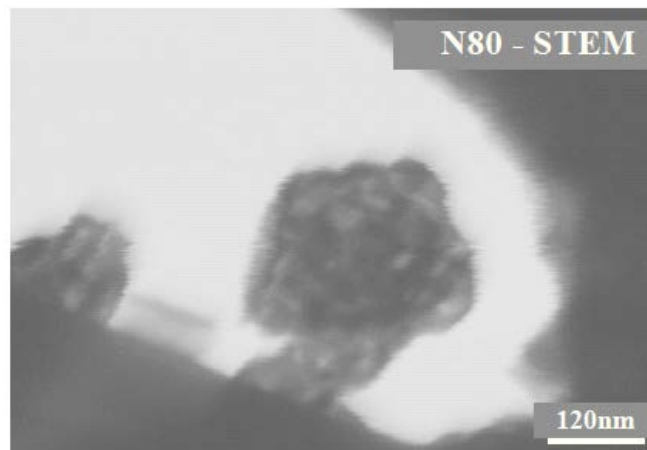


**Figure 4:** CaO nanostructure identified by TEM microscopy

References:

- [1] P. Suominen, P. Sortais, T. Stora, O. Tarvainen, Plasma Ion Sources for  $1^+$  molecular radioactive ion beams, ARIS 2011, Leuven, <https://iks32.fys.kuleuven.be/indico/contributionDisplay.py?contribId=194&confId=0>, accessed Feb 2012.
- [2] F. Schwellnus et al., Rev. Sci. Instrum. 81, 02A515 (2010).
- [3] J. P. Ramos, Effect of Calcium Oxide Microstructure on the Diffusion of Isotopes, CERN-THESIS-2012-008, <http://cdsweb.cern.ch/record/1425438?ln=en>

*A. Gottberg, T. Stora*

## The Dual RILIS:

### **RILIS**

Through the use of highly selective and efficient stepwise resonant ionization schemes, the ISOLDE RILIS has so far been applied for ionizing 28 of the elements produced at ISOLDE. The unique element selectivity of the laser ion source complements the mass selection process of the ISOLDE separator magnets to provide high purity ion beams of the chosen isotope. RILIS operation is requested by the users for over 2000 hours per year, amounting to over 50% of the total ISOLDE beam-time.

### **The RILIS dye laser system**

The RILIS comprises three dye lasers that can be focused and overlapped at a distance of ~20 m into the ionizer tube at the ISOLDE target. Up to three days of preparation are needed for a change from one element to another, this includes replacement of the dye solution (more than ten different organic dyes are used), laser set-up and alignment of the beams into the source. The RILIS dye laser system has been significantly improved since its first demonstration of selective ionization of radioactive Yb isotopes in 1992 [1]. In recent years the system has been progressively upgraded: The copper vapor pump laser was replaced by commercial solid-state diode pumped Nd:YAG lasers in 2009 and the home-built dye lasers were exchanged with state of the art commercial versions in 2010. [2]

### **A Complementary Laser system**

During 2011 a second independent laser system based on Nd:YAG pumped tunable titanium:sapphire (Ti:Sa) lasers was installed alongside the RILIS dye laser system. It offers great potential in meeting

the increasing demand for RILIS beams. This complementary laser setup enables the use of the many already established ionization schemes that require wavelengths produced by Ti:Sa lasers. Additionally, since the two systems can be used either independently or in combination with each other, the flexibility for switching from one ionization scheme to another is greatly improved. The main benefits are:

- Reduced switching time from one element to another
- Increased range of accessible elements
- Higher ionization efficiency due to increase in laser power (dye + Ti:Sa) and wider tuning range
- The solid-state nature of the Ti:Sa reduces maintenance work (no dye change)

The RILIS Ti:Sa system comprises two commercial 60 W frequency doubled Nd:YAG pump lasers and three broadly tunable solid-state Ti:Sa lasers. The laser parameters (10 kHz repetition rate, 5 W maximum output power and spectral line width of ~5 GHz) are well adapted to the RILIS requirements. The basic cavity design was adopted from the University of Mainz. The Ti:Sa laser setup was developed further by the RILIS team for improved operation in on-line conditions where time for setup and alignment is limited [3].

For the implementation of the new laser system without jeopardizing a successful restart of the RILIS dye laser system, the limited space inside the RILIS cabin was the biggest challenge. The layout of the RILIS was rearranged during the shut-down period 2010/11. Two additional optical tables and the obligatory laser safety screening were installed. A schematic view is shown in Fig.1.

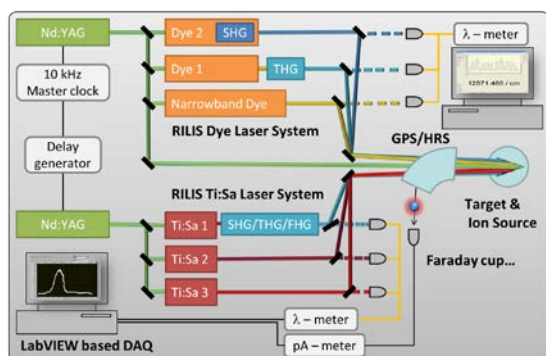


**Fig 1.** Schematic view of the upgraded RILIS laser setup.

### New modes of operation - The Dual RILIS

In 2011 RILIS was used on-line for a record time of 2757 h (184 h for TISD), producing ion beams of 16 different elements. For comparison, in 2010 the RILIS ON time amounted 2096 h. New modes of RILIS operation were investigated and some were already successfully used to provide beams to ISOLDE users. In the '*Ti:Sa only*' mode up to 50 W of the Nd:YAG dye pump laser is available for non-resonant ionization providing highest efficiencies (tested for Pr, Tl and Yb). For the '*mixed mode*' both laser systems (dye and Ti:Sa) are synchronized and work together. The laser type is chosen depending on the highest efficiency in the required wavelength range (demonstrated for Ag and At). In '*backup mode*' both systems could provide the same wavelength. In the case for Ni the Ti:Sa system was used to produce the final ionization step resulting in twice the ionization efficiency of the '*dye only*' setup. In the case for Zn the first step wavelength was obtained by both laser systems simultaneously i.e. four beams of three different wavelengths were transmitted to the ionizer tube. This enabled 3<sup>rd</sup> and 4<sup>th</sup> harmonics generation under reliable conditions, reducing damage to the nonlinear crystals and thus minimizing

down-time for users, whilst maintaining the same efficiency.

### In-source spectroscopy

Having a second laser system in place allowed for opportunistic use of ISOLDE beamtime. The Ti:Sa system was used for in-source spectroscopy using a Faraday cup to detect ions. Such micro-beamtimes were scheduled mainly during REX setup when the central beam line was in use and no other user could take beam from an operational target. This spectroscopy work resulted in the first experimental and precise measurement of the ionization potential of the astatine atom (article in preparation). The newly available efficient ionization scheme for astatine enables further in-source laser spectroscopy work to investigate the isotope shifts and hyperfine splittings as well as the continuation of the successful experiments for beta-delayed fission [4] for the astatine isotopes.

### References:

- [1] V.I. Mishin et al., Nucl. Instrum. and Meth. Phys. Research B 73, 550 (1993)
- [2] V.N. Fedosseev et al., Rev. Sci. Instrum. 83, 02A903 (2012).
- [3] S. Rothe et al., in J. Phys. Conf. Ser., Vol. 312 (IOP Publishing, 2011) p. 052020.
- [4] A. Andreyev et al., Phys. Rev. Lett. 105, 1 (2010).

*S. Rothe, V. Fedosseev, B. Marsh*

## TSR at HIE-ISOLDE Project:

### TSR@HIE-ISOLDE Collaboration

In 2011, after a positive evaluation of the Letter of Intent for installing a storage ring facility TSR at HIE-ISOLDE [1], our collaboration (see Ref. [2]) has prepared a full-scale Technical Design Report which has been submitted to the INTC in January 2012 [2]. If approved, we will build the first storage ring coupled to an ISOL-type radioactive beam facility. Such a facility will provide a capability for experiments with stored secondary beams that is unique in the world. The envisaged physics programme is rich and varied, spanning from investigations of nuclear ground-state properties and reaction studies of astrophysical relevance, to investigations with highly-charged ions and pure isomeric beams. In addition to experiments performed using beams recirculating within the ring, cooled beams can also be extracted and exploited by external spectrometers for high-precision measurements. A detailed description of the proposed physics cases can be found in Refs. [1,2].

Several options have been considered for the installation of TSR at ISOLDE. The scenario which was found to be the optimal is the installation of the ring in a new building located at the back (west side) of the ISOLDE experimental hall (see Figure). The floor of the new building would approximately be 2.8 m above the floor of the existing hall due to an essential infrastructure tunnel preventing the ring to be at equal height of the transfer beam line. To deliver the beams from the HIE-ISOLDE to the TSR a tilted beam line will have to be designed. The planned building will allow for installation of external setups which would profit from slowly-extracted electron-cooled beams.

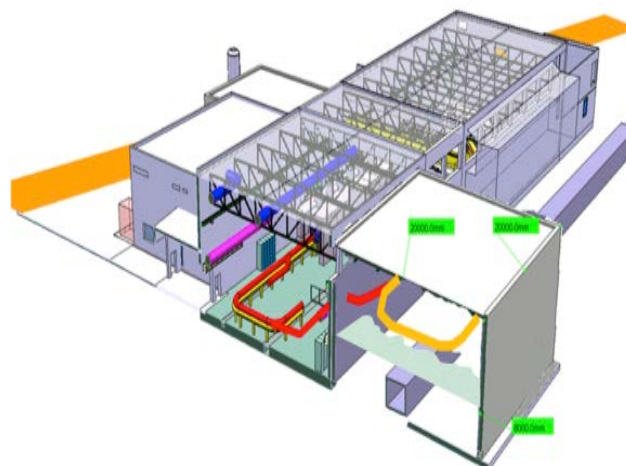


**Figure 1.** A possible location of the TSR storage ring at the HIE-ISOLDE.

The operation of the TSR at Max-Planck Institute for Nuclear Physics in Heidelberg will be stopped in the end of 2012. It is expected, that once the new building is available, the transport, reassembly and commissioning of the ring at ISOLDE can be accomplished within about 15 months.

In order to pursue the physics goals aimed at within the TSR@HIE-ISOLDE Project, several R&D studies have to be done. Therefore, a number of dedicated working groups have been formed. The TSR@HIE-ISOLDE is an open collaboration which invites all interested researchers to help us exploring the extremely rich scientific potential of the envisaged TSR@HIE-ISOLDE facility.

[1] A. Andreyev et al., Letter of Intent, CERN-INTC-2011-019 / INTC-I-133 (2011).

[2] M. Aliotta et al., Proposal, CERN-INTC-2012-027 / INTC-O-014 (2012).

*Y. Litvinov for the TSR at HIE-ISOLDE Collaboration*

## How to obtain access to the ISOLDE hall

1. Register at the CERN Users office<sup>1</sup>. You need to bring
  - a. [Registration form](#) signed by your **team leader or deputy**<sup>2</sup>
  - b. Proof of attachment<sup>3</sup> to Institute or University **in English or French**
  - c. Passport
  - d. Copy of medical insurance (for illness, private accidents, and work accidents and disability arising from such accidents at CERN)

2. Get your CERN access card in [Building 55](#)

With this registration procedure you become a **CERN user**<sup>4</sup>.

3. Follow the CERN basic safety course (levels 1 to 3):
  - a. If you have a CERN account, you can access the Safety Awareness course on-line at the web page <http://sir.cern.ch>, from your computer, inside or outside CERN.
  - b. If you have not activated your CERN account, there are some computers available for use without the need to log in on the first floor of building 55 (Your CERN badge will be needed in order to prove your identity).
4. Follow the radiation protection course only if you need to get a permanent personal dosimeter<sup>5</sup>. Please make a reservation for the course via EDH

- (CERN Electronic Document Handling) well in advance of your arrival at CERN<sup>6</sup>.
5. Obtain a radiation dosimeter at the Dosimetry service, located in [Building 55](#)<sup>7</sup>. Two options exist:
    - a. Temporary dosimeter. Issued only once per calendar year for a maximum of 2 months.
    - b. Permanent dosimeter. A [medical certificate](#)<sup>8</sup>, valid for 24 months, is required. The permanent dosimeter needs to be readout monthly<sup>9</sup>.
  6. Apply for access to ISOLDE hall using EDH:  
<https://edh.cern.ch/Document/ACRO>. This can be done by any member of your collaboration (typically the contact person) having an EDH account<sup>10</sup>.

Find more details at the [information about registration for Users](#) page.

New users are also requested to visit the ISOLDE User Support office while at CERN.

Opening hours:

Mon., Tues., Thurs., Fri. 08:30-12:30

Mon. & Thurs. 13:30-15:30

You can also use the summary "[Registration and ISOLDE access](#)" flow-chart as guidance.

---

<sup>1</sup> <http://cern.ch/ph-dep-UsersOffice> ([Building 61](#), open 8:30-12:30 and 14:00-16:00, closed Wednesday morning).

<sup>2</sup> Make sure that the registration form is signed by your team leader before coming to CERN or that it can be signed by the team leader or deputy upon arrival.

<sup>3</sup> Proof of attachment to Institute or University should not be signed by the person nominated as your team leader.

<sup>4</sup> The first registration as USER needs to be done personally, so please note the opening hours. If needed the extension of the registration can be delegated or performed on-line via EDH.

<sup>5</sup> The radiation protection course is mandatory to obtain a permanent personal dosimeter.

---

<sup>6</sup> If it is not possible to sign up for a course, a temporary dosimeter can be issued for the first registration at CERN.

<sup>7</sup> <http://cern.ch/service-rp-dosimetry> (open *only in the mornings* 08:30 - 12:00).

<sup>8</sup> The medical certificate must be brought in person to the Dosimetry Service (either by the user or a representative)

<sup>9</sup> There are reader stations at the ISOLDE hall and the CERN main building. You can leave your *permanent dosimeter* in the rack outside the ISOLDE User Support office.

<sup>10</sup> Eventually you can contact Jenny or the Physics coordinator.

## Contact information

### ISOLDE User Support

Jenny Weterings

[Jennifer.Weterings@cern.ch](mailto:Jennifer.Weterings@cern.ch)

+41 22 767 5828

### Chair of the ISCC

Maria Jose G<sup>a</sup> Borge

[borge@iem.cfmac.csic.es](mailto:borge@iem.cfmac.csic.es)

+34 91 59 01 614

### Chair of the INTC

Peter Butler

[peter.butler@liverpool.ac.uk](mailto:peter.butler@liverpool.ac.uk)

+44 151 794 3443

### ISOLDE Physics Section Leader

Yorick Blumenfeld

[Yorick.Blumenfeld@cern.ch](mailto:Yorick.Blumenfeld@cern.ch)

+41 22 767 5825

### ISOLDE Physics Coordinator

Magdalena Kowalska

[Magdalena.Kowalska@cern.ch](mailto:Magdalena.Kowalska@cern.ch)

+41 22 767 3809

### ISOLDE Technical Coordinator

Richard Catherall

[Richard.Catherall@cern.ch](mailto:Richard.Catherall@cern.ch)

+41 22 767 1741

### HIE-ISOLDE Project Leader

Yacine Kadi

[Yacine.Kadi@cern.ch](mailto:Yacine.Kadi@cern.ch)

+41 22 767 9569

More contact information at

<https://isolde.web.cern.ch/ISOLDE/default2.php?index=index/groupindex.htm&main=group/contacts.php> and at

<https://isolde.web.cern.ch/ISOLDE/default2.php?index=index/groupindex.htm&main=group/places.php>

